

Article

Organic Matter Assessment and Paleoenvironmental Changes of the Middle Jurassic Main Source Rocks (Khatatba Formation) in the North Western Desert, Egypt: Palynofacies and Palynomorph Perspectives

Ahmed Mansour ^{1,2,3}, Sameh S. Tahoun ⁴, Aya Raafat ⁴, Mohamed S. Ahmed ⁵, Francisca Oboh-Ikuenobe ⁶, Thomas Gentzis ^{7,*} and Xiugen Fu ^{1,2}

- ¹ State Key Laboratory of Oil and Gas Reservoir Geology and Exploitation, Southwest Petroleum University, Chengdu 610500, China; ahmedmans48@mu.edu.cn (A.M.)
 - ² School of Geoscience and Technology, Southwest Petroleum University, Chengdu 610500, China
 - ³ Geology Department, Faculty of Science, Minia University, Minia 61519, Egypt
 - ⁴ Geology Department, Faculty of Science, Cairo University, Giza 12613, Egypt; stahoun@cu.edu.eg (S.S.T.); ayar210@yahoo.com (A.R.)
 - ⁵ Geology and Geophysics Department, College of Science, King Saud University, Riyadh 11451, Saudi Arabia; mohammed@ksu.edu.sa
 - ⁶ Department of Geosciences and Geological and Petroleum Engineering, Missouri University of Science and Technology, Rolla, MO 65409, USA; ikuenobe@mst.edu
 - ⁷ Core Laboratories, 6316 Windfern Road, Houston, TX 77040, USA
- * Correspondence: thomas.gentzis@corelab.com



Citation: Mansour, A.; Tahoun, S.S.; Raafat, A.; Ahmed, M.S.; Oboh-Ikuenobe, F.; Gentzis, T.; Fu, X. Organic Matter Assessment and Paleoenvironmental Changes of the Middle Jurassic Main Source Rocks (Khatatba Formation) in the North Western Desert, Egypt: Palynofacies and Palynomorph Perspectives. *Minerals* **2023**, *13*, 548. <https://doi.org/10.3390/min13040548>

Academic Editor: Leszek Marynowski

Received: 8 March 2023

Revised: 7 April 2023

Accepted: 10 April 2023

Published: 13 April 2023



Copyright: © 2023 by the authors. Licensee MDPI, Basel, Switzerland. This article is an open access article distributed under the terms and conditions of the Creative Commons Attribution (CC BY) license (<https://creativecommons.org/licenses/by/4.0/>).

Abstract: The Middle Jurassic in the north Western Desert, Egypt, was a time of complex tectonics and increased environmental perturbations attributed to the predominant sedimentation of organic carbon-rich fine siliciclastic and carbonate deposits of the Khatatba Formation. Although some studies have addressed the hydrocarbon potential and source rock characteristics of the Khatatba Formation, a regional-scale investigation of the prevalent paleoenvironmental conditions and organic matter characteristics is still necessary. In this study, the Khatatba Formation is investigated for detailed palynofacies analysis and palynomorph composition to assess organic matter kerogen types and reconstruct the depositional paleoenvironmental patterns on a regional scale. For this purpose, 116 drill cuttings were collected from five wells in the Matruh, Shushan, and Dahab-Mireir Basins. Moderately diverse assemblages of spores, pollen, and dinoflagellate cysts are reported. Age-diagnostic dinoflagellate cysts, including *Adnatosphaeridium caulleryi*, *Dichadogonyaulax sellwoodii*, *Korystocysta gochtii*, *Wanaea acollaris*, and *Pareodinia ceratophora*, along with occasional records of *Systematophora areolate* and *Systematophora penicillate*, defined a Bajocian–Callovian age. Based on particulate organic matter (POM) composition, four palynofacies assemblages (PFAs) are identified. PFA-1 is the most common within the Khatatba Formation in the five studied wells. It contains high proportions of phytoclast fragments versus low contents of amorphous organic matter (AOM) and palynomorphs and is defined by a gas-prone kerogen Type III. PFA-2 is comprised of moderate abundances of AOM and phytoclast characteristics of oil-prone kerogen Type II. PFA-3 is dominated by phytoclasts and moderate to low proportions of AOM and palynomorphs of kerogen Type III, whereas PFA-4 consists of AOM and palynomorphs defining kerogen Type II. PFA-1 indicates predominant deposition in proximal active fluvio-deltaic sources to marginal marine conditions with enhanced contributions of terrestrial/riverine influx. PFA-2 and PFA-3 reveal deposition under an enhanced dysoxic to anoxic proximal inner neritic shelf due to the abundant occurrences of spores and coastal to shallow marine dinoflagellate cysts. PFA-4 suggests deposition under enhanced suboxic to anoxic distal inner neritic conditions because of enhanced AOM and abundant proximate and some chorate dinoflagellate cysts. Thus, the Middle Jurassic experienced a predominantly marginal to shallow water column in this part of the southern margin of the Tethyan Ocean where the Matruh, Shushan, and Dahab-Mireir Basins were located.

Keywords: organic matter characterization; kerogen types; palynomorph composition; Matruh Basin; Shushan Basin; Dahab-Mireir Basin

1. Introduction

A long-term rise in the eustatic sea level during the Middle Jurassic (Bathonian–Callovian) is believed to be close to or below the present-day mean sea level [1]. This resulted in the deposition of thick siliciclastic–carbonate intervals with organic-matter-rich strata in the southern margin of the Tethys Ocean where the north Western Desert in Egypt is located [2]. The north Western Desert is considered one of the most promising provinces for petroleum exploration and production activities in all of Egypt. Several outstanding oil and gas discoveries have been successfully made in the last two decades that enhance considerable reserve estimates, especially in giant sedimentary basins such as the Shushan, Abu Gharadig, and Matruh Basins [2–6] (Figure 1). Another important reason is that these basins have thick stratigraphic successions that range from 7600 m to 9000 m at their basin depocenters [2–7].

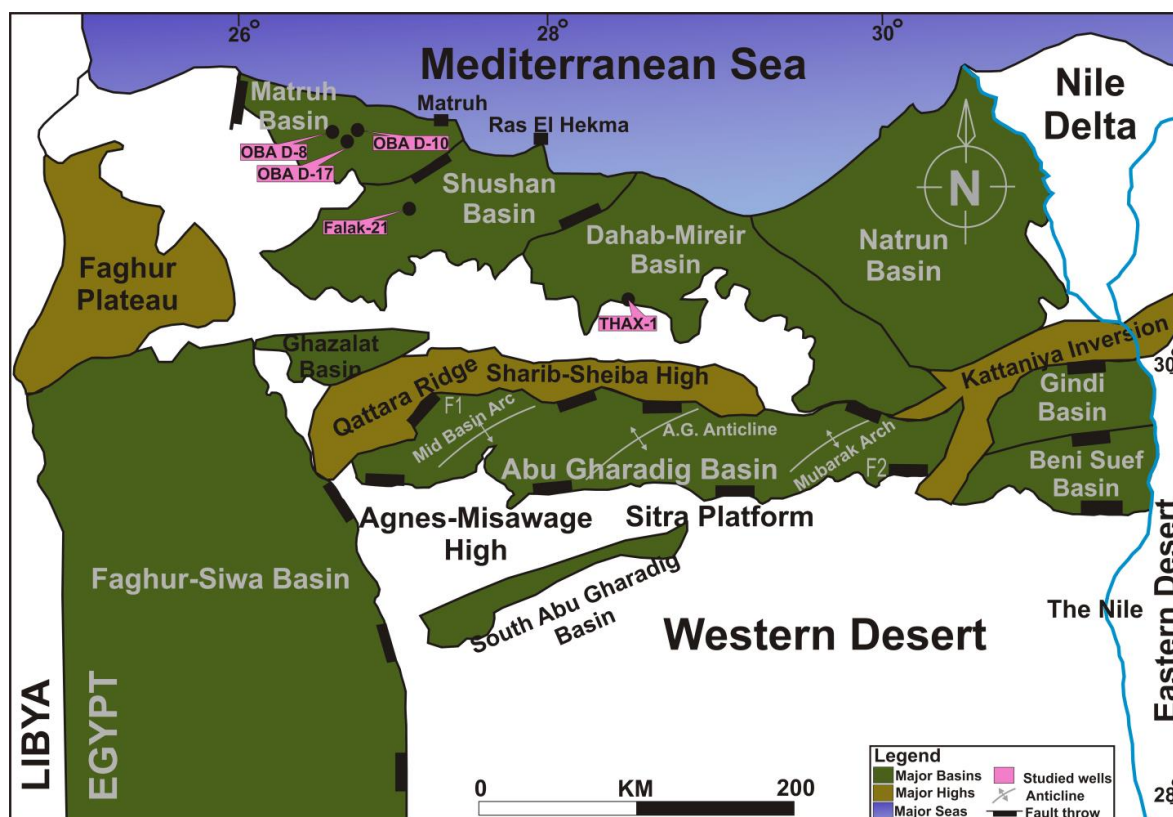


Figure 1. Major sedimentary basins, adjoining highs, and controlling structures of the north Western Desert (modified after EGPC [2]). The locations of the current study wells are also shown.

The Khatatba Formation is the main source rock unit in the north Western Desert [2,4,5,8]. Although several organic geochemical investigations of the Khatatba Formation have assessed source rock potential and organic matter characteristics, the degree of thermal maturity and burial history [3–5,8–11] and detailed palynomorph and palynofacies analyses are lacking in this region of the Western Desert.

Palynomorph composition and palynofacies analysis are among the techniques used by several oil companies and research institutes for reliable biostratigraphic assessment of relative age dating of sedimentary strata as well as visual evaluation of preserved organic matter quality and thermal maturity. Palynofacies analysis includes all organic

components recovered from sediments, such as opaque (equidimensional and lath-shaped) and translucent phytoclasts (wood tracheids, cuticles, fungal hyphae, and membranes), amorphous organic matter (AOM, including biodegraded AOM), and palynomorphs (i.e., spores, pollen, freshwater algae, dinoflagellate cysts, acritarchs, microforaminiferal test linings (MFTLs), and prasinophytes), all of which are known as particulate organic matter (POM) [12,13]. Palynofacies analysis addresses the relative proportions of POM components in an absolute representation and their preservation states. Therefore, it assists in the reliable assessment of organic matter characteristics with respect to different types of kerogen quality and quantity, especially when the studied rock units have a petroleum-generating potential, as is the case of the Middle Jurassic Khatatba Formation.

In this paper, the results of extensive palynomorph and palynofacies analyses of the Khatatba Formation in the Falak-21, THAX-1, OBA D-8, OBA D-10, and OBA D-17 wells are presented to achieve the following: (1) assess the types of kerogen from palynofacies characteristics in order to predict the expected types of expelled hydrocarbons and compare the results of palynofacies analysis with reliable Rock-Eval hydrogen index (HI) results from available previous studies; and (2) reconstruct short-term changes in environmental conditions at the time of deposition of the Khatatba Formation in the Shushan, Matruh, and Dahab-Mireir Basins based on palynofacies analysis and palynomorph components.

2. Geologic Setting

The north Western Desert is located at the extreme northeastern margin of the African Plate, and thus it was subjected to complex tectonic evolution from the Paleozoic to the Cenozoic when several extensional-rift basins were developed [14]. These include the Matruh, Shushan, Natrun, and Dahab-Mireir Basins in the coastal parts of the north Western Desert and the Abu Gharadig, Gindi, and Beni-Suef Basins towards the south (Figure 1), which were all located in the southern Tethyan passive margin [15,16]. The current study areas are in the Matruh, Shushan, and Dahab-Mireir Basins (Figure 1). The location of these basins in the northern part of Egypt is commonly known as the unstable shelf [17]. Rifting in northern Egypt was affected by multiple regional tectonic events. During the Permo–Triassic to Liassic, active extensional forces took place in response to the breakup of Gondwana and consequently, the opening of the Neo-Tethys Ocean [14,18]. During the Middle Jurassic, when the activation of the late Cimmerian Orogeny occurred, the Apulian microplate separated from the NE African (i.e., Egypt) territory and rifted northward [19]. This was accompanied by the eastward movement of the African Plate relative to the European Plate with respect to the opening of the Atlantic Ocean [20,21]. These regional tectonics led to the formation of several NNE–SSW extensional rift basins, including the basins of interest in this study, as evidenced by NE–SW oriented major faults in the subsurface structural data from the north Western Desert [16,22,23]. These major faults controlled the subsidence rates of the main basinal blocks of the Matruh, Shushan, and Dahab-Mireir Basins.

During the Late Cretaceous, major compressional episodes were controlled by enhanced convergence between the African and Eurasian Plates, which reached maxima by the Santonian to Paleogene [14,21,23]. These structural episodes resulted in the formation of an ENE–WSW trending fold belt across northern Egypt, the so-called Syrian Arc System [22,24]. These consequential tectonic events and complex structural settings in northern Egypt created multiple, well-developed petroleum systems within the sedimentary record of the Matruh and Shushan Basins [2].

Major normal faults separate the Matruh, Shushan, and Dahab-Mireir Basins, which are bounded by the Natrun Basin to the east, the Faghur-Umbarka Platform to the west, the Mediterranean Sea to the north, and the Qattara Ridge and Sahrib-Sheiba High to the south (Figure 1). The three basins contain thick stratigraphic successions that are in the range of 7500–9000 m thick at the basin center. The Matruh Basin is a broad downwarp bounded by NNE–SSW trending normal faults. The Shushan Basin is a collapsed crest with multiple inversion anticlines (trending NNE–SSW and NE–SW) and tilted fault blocks

separated by normal faults (trending NW–SE and WNW–ESE) [22]. The Dahab-Mireir Basin represents the central remnant of the major coastal area with a northeastward trend, which is bifurcated with a SE extension. Additionally, two ridges (trending ENE) of the Qattara-Alamein and Washka cut this basin [22].

The stratigraphic successions of the Matruh, Shushan, and Dahab-Mireir Basins are generally similar and consist of Permo–Triassic to Miocene alternations of siliciclastic sediments and carbonate facies (Figure 2).

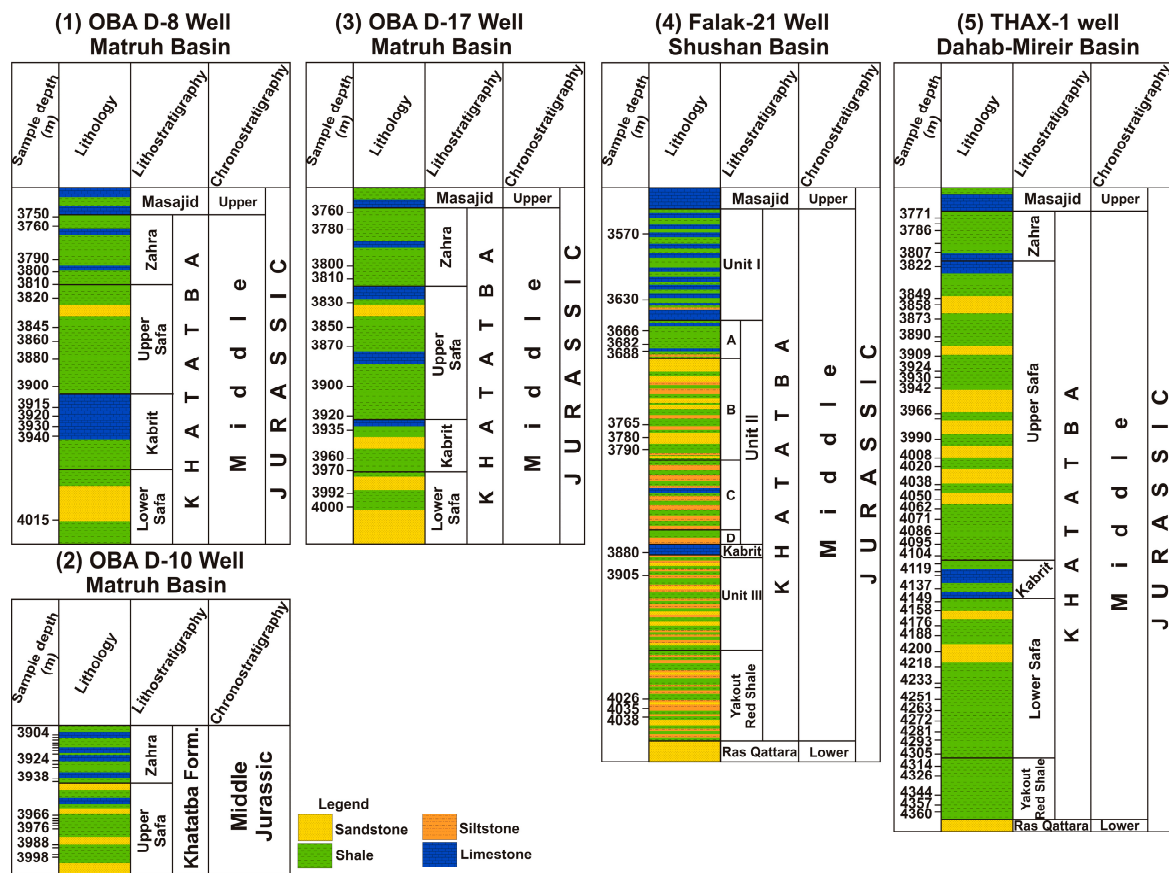


Figure 2. Lithostratigraphic successions of the Middle Jurassic Khatatba Formation in the OBA D-8, OBA D-10, and OBA D-17 wells in the Matruh Basin [6], the Falak-21 well in the Shushan Basin [5], and the THAX-1 well in the Dahab-Mireir Basin in the north Western Desert, Egypt [6]. Representative depths of each sample are also shown.

This study focuses on the Middle Jurassic Khatatba Formation in the OBA D-8, OBA D-10, and OBA D-17 wells in the Matruh Basin, the Falak-21 well in the Shushan Basin, and the THAX-1 well in the Dahab-Mireir Basin (Figures 1 and 2). The Khatatba Formation was established by Norton [25] and the type section was described in the Khatatba-1 well [2]. The formation conformably overlies the Lower Jurassic siliciclastic sediments of the Ras Qattara Formation and conformably underlies the Upper Jurassic Masajid Formation. The Khatatba Formation is composed of organic carbon-rich black to dark brown shales intercalated with thin white and brown medium-grained sandstones, fine siltstones, and coaly shales, along with several limestone interbeds (Figure 2). It changes vertically into the carbonate sediments of the Masajid Formation. During the Lower-Middle Jurassic, a phase of gradual marine transgression took place in northern Egypt and led to the deposition of major clastics and carbonate facies, such as the Ras Qattara and Khatatba formations.

3. Materials and Methods

A total of 116 drill cuttings representing the Khatatba Formation in the OBA D-8, OBA D-10, OBA D-17, Falak-21, and THAX-1 wells in the Matruh, Shushan, and Dahab-Mireir Basins of the north Western Desert, Egypt, were used for detailed palynomorph investigation and palynofacies analysis. The number of cuttings and depth intervals, along with the longitude and latitude of each well, are summarized in Table 1.

Table 1. Longitudes and latitudes of the current study wells in the north Western Desert as well as the number of representative samples selected from the Khatatba Formation in each well.

Well Name	Longitude	Latitude	Sedimentary Basin	Number of Samples	Depth Interval (m)
OBA D-8	26°35'6.32" E	31°05'41.68" N		15	3750–4015
OBA D-10	26°41'50.67" E	31°07'31.60" N	Matruh	23	3904–3998
OBA D-17	26°40'2.09" E	31°4'5.28" N		14	3760–4000
Falak-21	27°0'14.75" E	30°48'45.16" N	Shushan	14	3570–4038
THAX-1	28°29'0.0" E	30°20'0.0" N	Dahab-Mireir	51	3771–4360

For each sample, an aliquot of 15 g was subjected to acid-based chemical processing of concentrated HCl (35%) to remove the carbonate fractions and HF (70%) to remove the silicate particles following the proposed procedures of Traverse [26]. The organic residue of each sample was sieved and cleaned in 15 µm nylon mesh, which was suspended onto a glass slide to dry. The slides were permanently mounted in Canada Balsam and a glass cover slip was placed. Generally, two glass slides were prepared for each sample and examined under transmitted white light. The slides for the Falak-21 well samples were examined using an OMAX ToupView microscope and a digital camera (SCMOS05000KPA) at the Micropalaeontology Laboratory, Geology Department, Faculty of Science, Minia University, Egypt. However, all the slides for the other four wells were examined using a BEL microscope and a TUCSEN camera and are stored at the Geology Department, Faculty of Science, Cairo University, Egypt. For qualitative and quantitative palynomorph and palynofacies analyses, a total of 200 palynomorph grains and 500 POM samples were counted, respectively. The detailed description of the kerogen groups used in this study is included as Figure S1 in Supplementary Materials.

4. Results

4.1. Palynomorph Composition

The Khatatba Formation in the five studied wells yielded a diverse assemblage of marine and terrestrial palynomorphs, including spores, pollen grains, dinoflagellate cysts, MFTLs, and acritarchs. An assemblage of 82 species of dinoflagellate cysts, spores, and pollen grains belonging to 46 genera were identified (Table S1). The dinoflagellate cysts are comprised of an abundant distribution of long-ranging marker species such as *Adnatosphaeridium caulleryi*, *Cribroperidinium* sp., *Ctenidodinium combazii*, *Dichadogonyaulax sellwoodii*, *Escharisphaeridia pocokii*, *Korystocysta gochtii*, *Korystocysta pachyderma*, *Lithodinia jurassica*, *Oligosphaeridium* sp., *Pareodinia ceratophora*, *Sentusidinium* sp., *Systematophora areolata*, *Systematophora complicata*, *Systematop hora* sp., and *Wanaea acollaris* (Figures 3 and 4).

The spore content is dominated by *Cicatricosisporites* sp., *Concavisporites* sp., *Cyathidites australis*, *Cyathidites minor*, *Deltoidospora minor*, *Deltoidospora* sp., *Dictyophyllidites* sp., *Gleicheniidites senonicus*, *Gleicheniidites* sp., *Impardecispora* sp., and *Microreticulatisporites uniformis* (Figure 5). The pollen grain content consists of *Araucariacites australis*, *Callialasporites dampieri*, *Callialasporites trilobatus*, *Cycadopites ovatus*, *Cycadopites* sp., *Ephedripites* sp., *Inaperturopollenites* spp., and *Spheripollenites psilatus* (Figure 4).

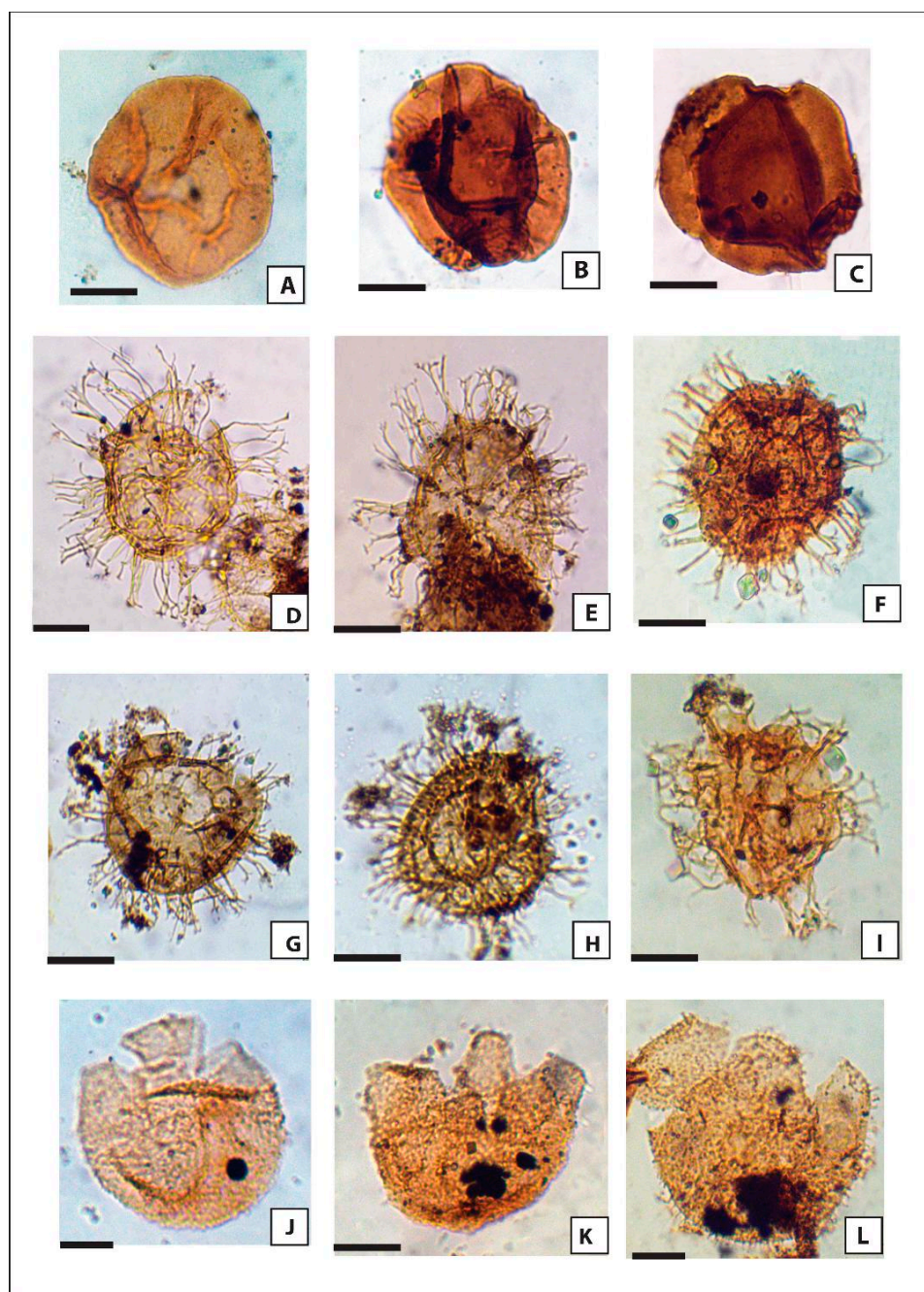


Figure 3. Photomicrographs of the recovered pollen grains and dinoflagellate cysts from the Khatatba Formation taken under transmitted white light. The corresponding well name, sample depth, slide number, and microscope coordinates of the species in the kerogen slides are given. The scale bar is equivalent to 30 μm . (A) *Araucariacites australis*, OBA D-8, 3820 m, slide 1, Coord. 41/11. (B,C) *Callialasporites trilobatus*, OBA D-8, 3810 m, slide 1, Coord. 35.5/11.5; OBA D-10, 3910 m, slide 2, Coord. 55/11. (D,E) *Systematophora penicillata*, Falak-21, 3682 m, slide 2, Coord. 33/10; OBA D-17, 3870 m, slide 1, Coord. 59/5.5. (F) *Systematophora areolata*, THAX-1, 3807 m, slide 1, Coord. 49/11.5. (G) *Systematophora complicata*, OBA D-8, 3790 m, slide 1, Coord. 59/5.5. (H,I) *Systematophora* sp., OBA D-10, 3916 m, slide 2, Coord. 55/10.5; THAX-1, 3777 m, slide 1, Coord. 33/9. (J,K) *Sentusidinium* sp., Falak-21, 3765 m, slide 2, Coord. 34/12; OBA D-17, 3800 m, slide 1, Coord. 41/10. (L) *Sentusidinium echinatum*, OBA D-17, 3830 m, slide 2, Coord. 31/10.

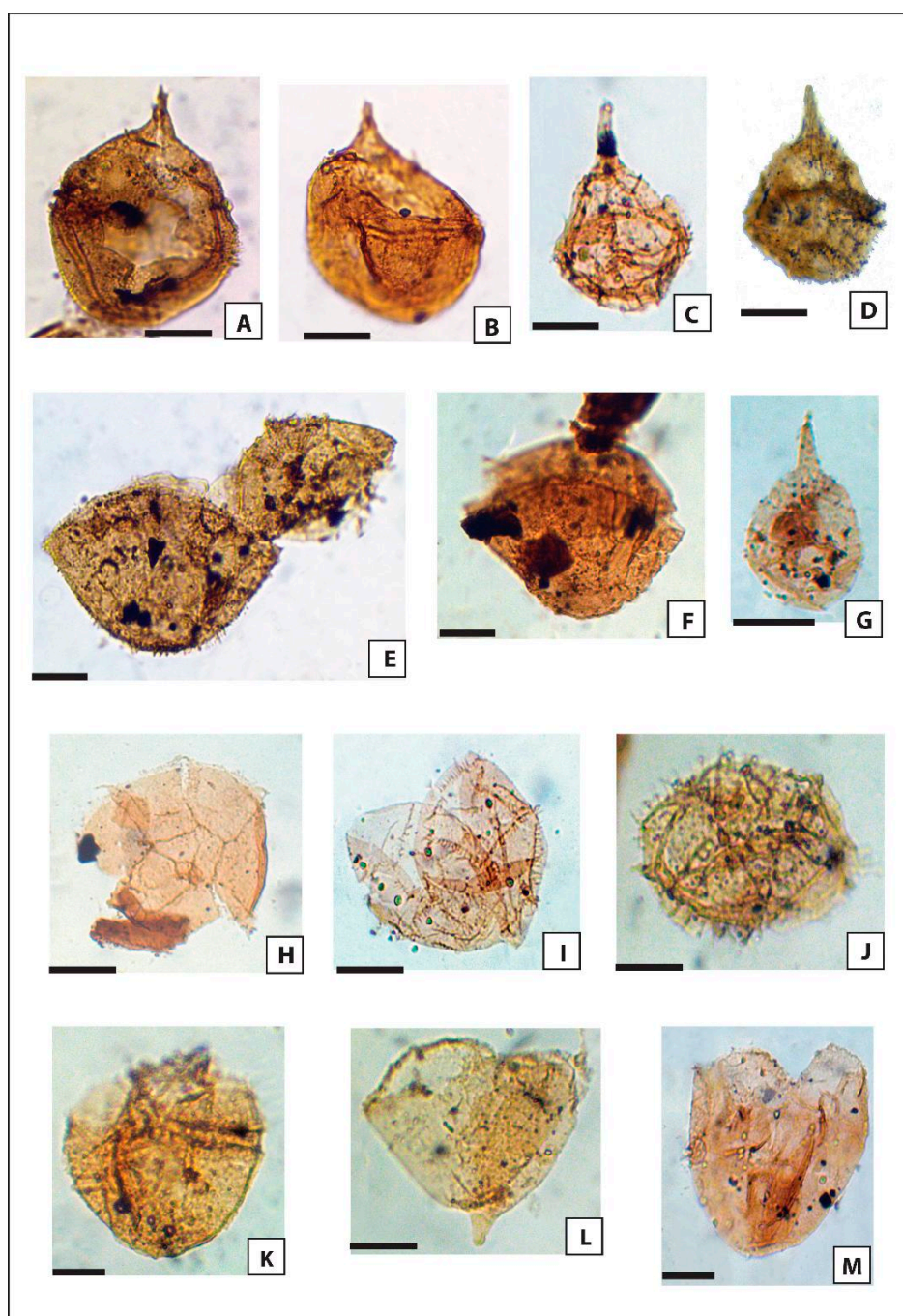


Figure 4. Photomicrographs of the recovered dinoflagellate cysts and microforaminiferal test linings from the Khatatba Formation taken under transmitted white light. The corresponding well name, sample depth, slide number, and coordinates of the species in the kerogen slides are given. The scale bar is equivalent to 30 μm . (A,B) *Cribooperidinium globatum*, OBA D-10, 3928 m, slide 1, Coord. 38.1/12; OBA D-8, 3820 m, slide 1, Coord. 34/8.5. (C) *Gonyaulacysta* cf. *adecta*, OBA D-10, 3910 m, slide 1, Coord. 44/4.5. (D) *Gonyaulacysta adecta* THAX-1, 3786 m, slide 1, Coord. 36/13.8. (E,F) *Korystocysta gochtii*, Falak-21, 3570 m, slide 1, Coord. 60/10; THAX-1, 3795 m, slide 1, Coord. 44/11. (G) *Pareodinia ceratophora*, OBA D-8, 3900 m, slide 1, Coord. 51/7.5. (H) *Dichadogonyaulax sellwoodii*, OBA D-10, 3940 m, slide 1, Coord. 56/11. (I) *Dichadogonyaulax* cf. *sellwoodii*, THAX-1, 3822 m, slide 2, Coord. 51/10. (J) *Ctenidodinium* cf. *combazii*, OBA D-17, 3760 m, slide 2, Coord. 50/8. (K) *Lithodinia jurassica*, Falak-21, 3682 m, slide 2, Coord. 33/17. (L) *Wanaea acollaris*, OBA D-17, 3800 m, slide 1, Coord. 48/14. (M) *Escharisphaeridia pocockii*, OBA D-8, 3800 m, slide 2, Coord. 55/17.5.

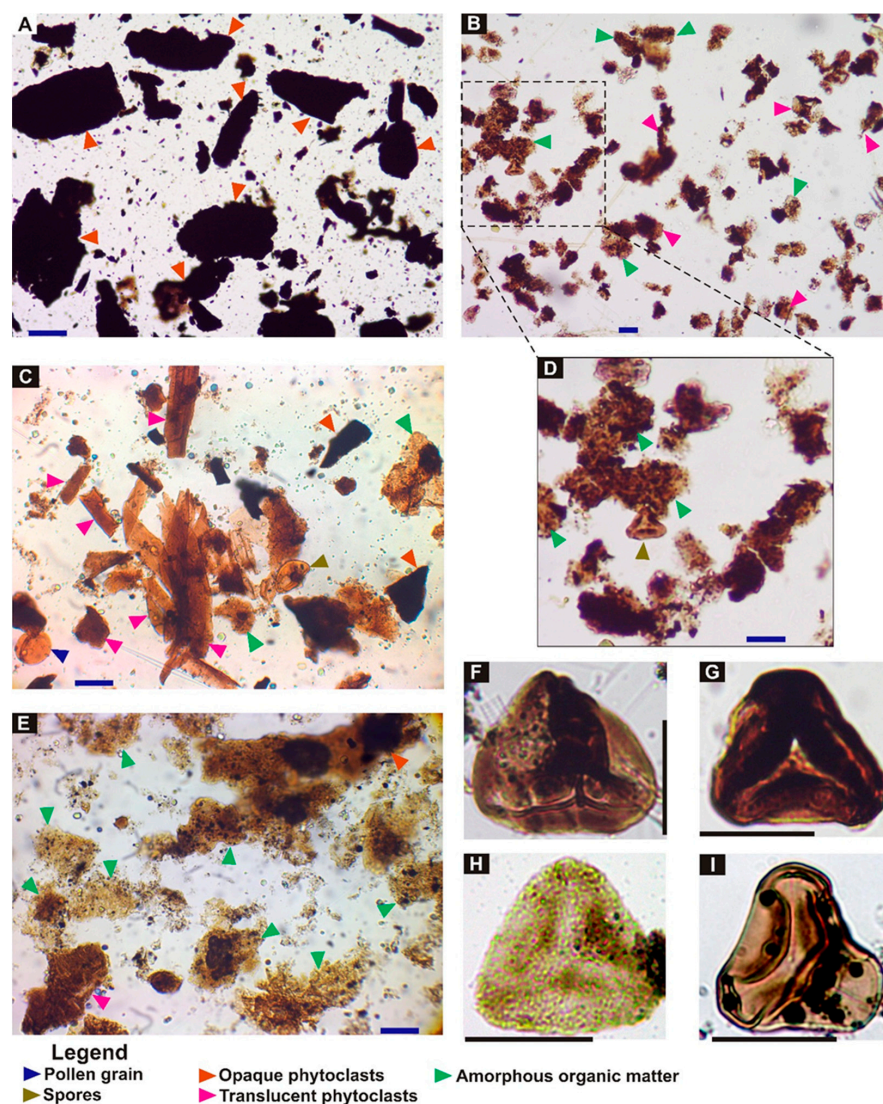


Figure 5. Photomicrographs of the recovered POM and spores from the Khatatba Formation taken under transmitted white light. The corresponding well name, sample depth, slide number, and coordinates of the species in the kerogen slides are given. The scale bar is equivalent to 40 μm . (A) POM composition of PFA-1 with high proportions of opaque phytoclast fragments in the Falak-21 well, 3905 m, slide 1; (B) POM composition of PFA-2 with moderate proportions of AOM and phytoclasts in the OBA D-17 well, 4000 m, slide 1; (C) POM composition of PFA-3 with moderate proportions of phytoclasts and AOM with enhanced palynomorphs in the THAX-1 well, 4119 m, slide 1; (D) exaggeration of POM composition of PFA-2 showing abundant AOM and translucent phytoclasts with a spore. (E) POM composition of PFA-4 with high concentration of AOM in the OBA D-8 well, 3790 m, slide 1; (F) *Deltoidospora hallii*, Falak-21, 3682 m, slide 1, Coord. 35/9; (G) *Dictyophyllidites* sp., THAX-1, 3858 m, slide 1, Coord. 40.7/11; (H) *Microreticulatisporites* sp., Falak-21, 3570 m, slide 2, Coord. 51.5/9.6; (I) *Gleicheniidites* sp., OBA D-10, 3928 m, slide 1, Coord. 37/8.7.

The Khatatba Formation samples exhibit significant stratigraphic records of various palynomorph groups and M:T ratios, which are shown in Figures 6 and 7. It is characterized by abundant palynomorph composition; however, the OBA D-17 well samples show zero to low numbers of spores and pollen grains, and the lowermost interval is barren. The Falak-21 samples exhibit a low yield of palynomorphs, except for the samples at depths of 3570 m, 3682 m, and 3765 m, which contain abundant palynomorphs. In the OBA D-8 well, spores are absent and pollen grains are sparsely recorded as absent, while dinoflagellate cysts are dominant, reaching up to a maximum average value of 97% of

total palynomorph composition. All the Khatatba Formation samples in the OBA D-10 and THAX-1 wells contain palynomorph-rich assemblages of spores, pollen grains, and dinoflagellate cysts. Low to rare records of MFTLs and acritarchs are reported within the formation in the OBA D-8, Falak-21, and THAX-1 wells. Due to abundant records of terrestrial and marine palynomorphs, a marine:terrestrial (M:T) ratio is calculated by subdividing the sum of marine palynomorph proportions (dinoflagellate cysts, MFTLs, and acritarchs) by terrestrial palynomorphs, including pollen grains and spores. The M:T ratios of the Khatatba Formation in the THAX-1 and Falak-21 wells are generally moderate to low and are in the range of 2–0.1 (0.5 on average) and 1.1–0 (0.5 on average), respectively. The highest M:T ratios are reported within the OBA D-8 well (up to 49) compared to OBA D-17 (up to 13.3) and OBA D-10 (up to 2.1), which exhibit lower average values of 5.2 and 2.1, respectively.

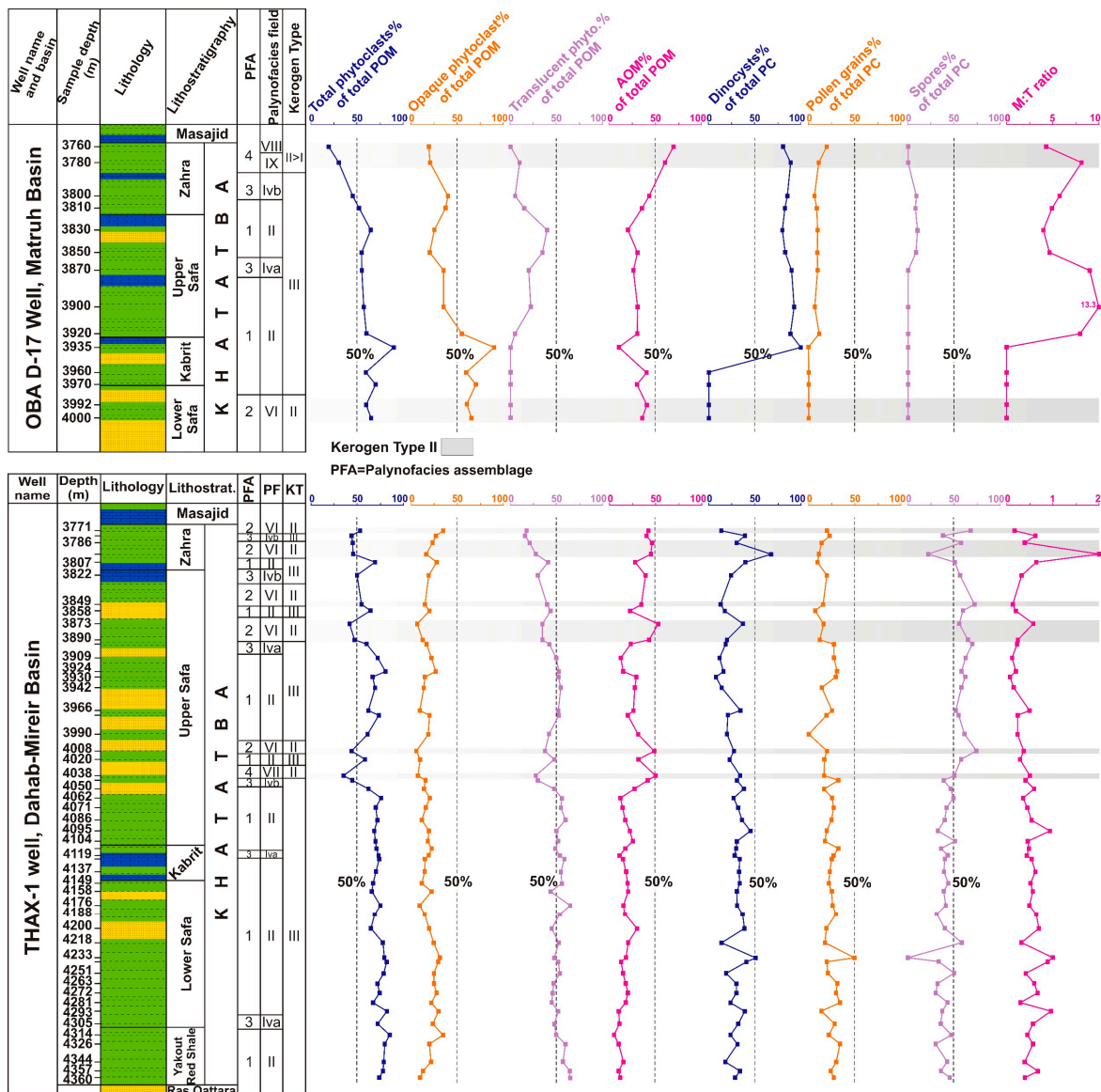


Figure 6. Stratigraphic distribution chart of kerogen parameters, palynomorph composition, and M:T ratios of the Khatatba Formation from the OBA D-17 and THAX-1 wells in the Matruh and Dahab-Mireir Basins, respectively.

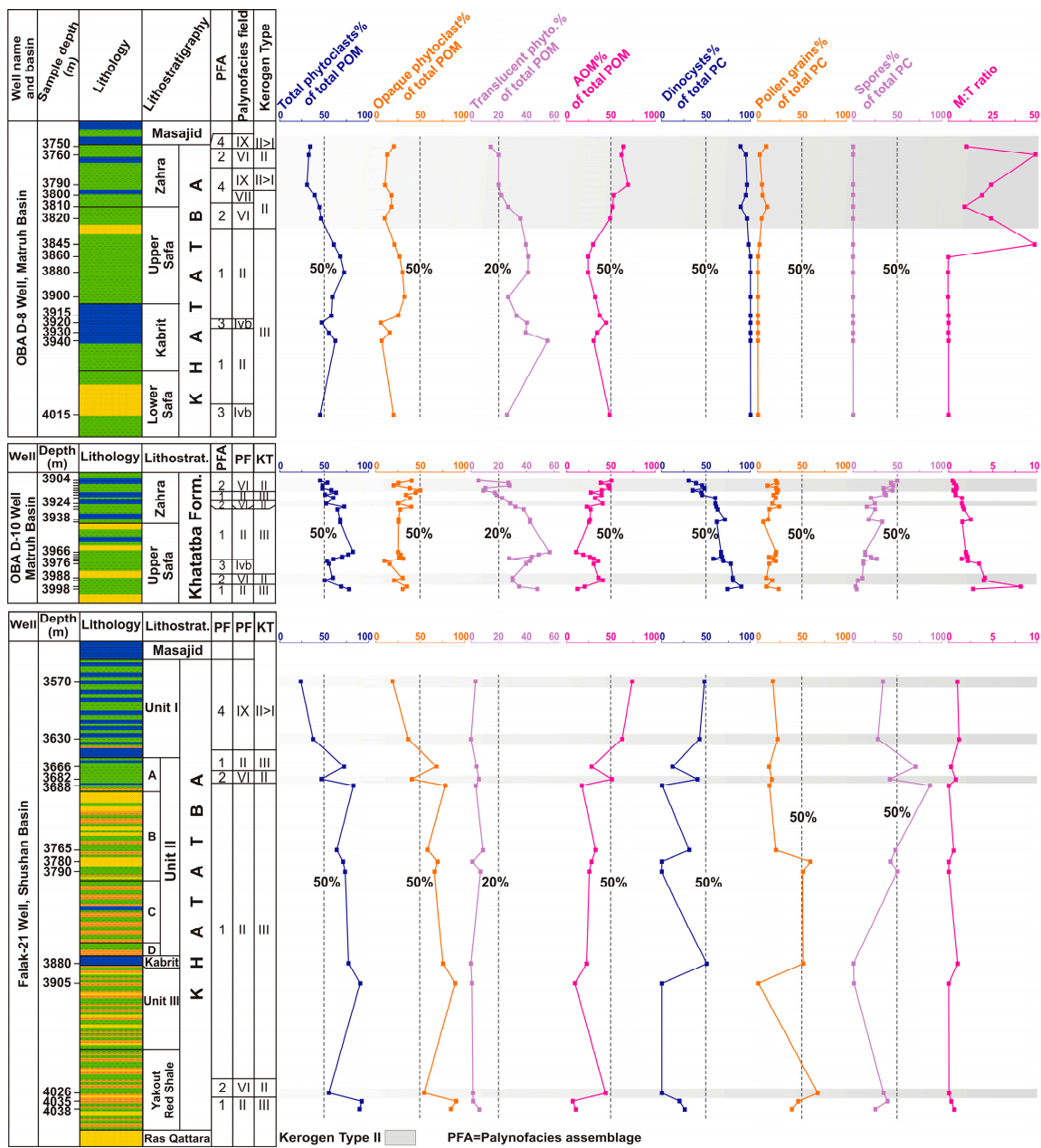


Figure 7. Stratigraphic distribution chart of kerogen parameters, palynomorph composition, and M:T ratios of the Khatatba Formation from the OBA D-8 and OBA D-10 wells in the Matruh Basin and the Falak-21 well in the Shushan Basin.

4.2. Palynofacies Analysis

The POM composition of the Khatatba Formation varies between the studied wells in the Matruh, Shushan, and Dahab-Mireir Basins, and is represented by variable concentrations of phytoclasts, AOM, and palynomorph compositions (Table S2). Based on palynofacies analysis of the stratigraphic change in POM composition, the Khatatba Formation samples can be discriminated according to their plot in the AOM-Phytoclasts-Palynomorphs (APP) ternary diagram of Tyson [12] (Figure 8). Therefore, the samples (Figures 6 and 7) are divided into four palynofacies assemblages (PFAs), which reveal the different kerogen types of preserved organic matter, the redox conditions, and the role of terrigenous influx at the time of deposition.

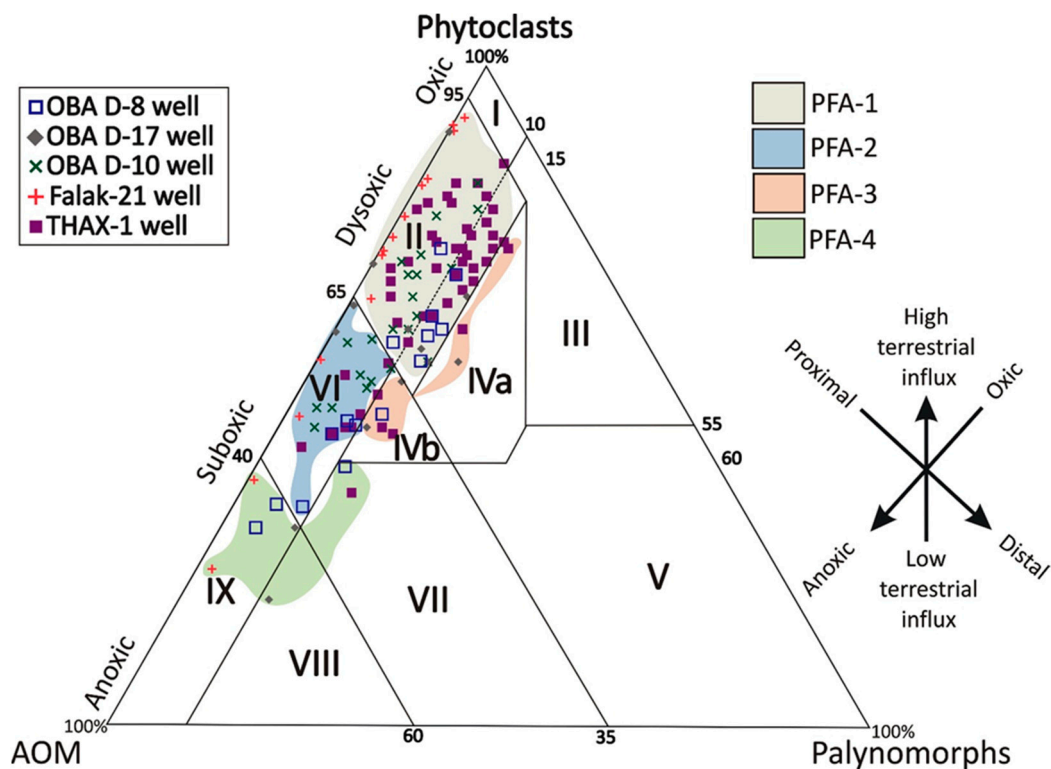


Figure 8. Ternary diagram of the three endmembers of AOM-Phytoclasts-Palynomorphs (APP, after [12]) shows the distribution of majority of the Khatatba Formation samples in the five studied wells in palynofacies fields II, IV and VI, and few samples plot in palynofacies fields IX and VIII.

Palynofacies assemblage 1 (PFA-1), the most common assemblage throughout the Khatatba Formation in the five studied wells, is represented by thirty-seven, fourteen, nine, eight, and seven samples from the THAX-1, OBA D-10, Falak-21, OBA D-17, and OBA D-8 wells, respectively (Table S2). The PFA-1 samples plot in palynofacies field II on the APP ternary diagram (Figure 8). This palynofacies assemblage is characterized by the highest contents of the total phytoclast particles compared to the lowest concentration of AOM and palynomorphs (Figure 5A). The highest phytoclast content (64.2%–92%) is reported within the Falak-21 well with an average of 79.2% of total POM composition dominated by opaque phytoclasts (56.2%–91.2%, 76.2% on average) compared to translucent phytoclasts (0%–8%, 3% on average) (Figure 8). The AOM in the Falak-21 well is in the range of 6.8%–32.6% (19.6% on average), while the average palynomorph composition is 1% of the total POM content. Unlike the Falak-21 well, the OBA D-8 well in the Matruh Basin preserves the lowest phytoclast contents (55%–72%, 62% on average) compared to the other studied wells (Figures 7 and 9) versus moderate AOM (20%–33%, 26.3% on average) and palynomorph contents (8%–14%, 11.7% on average). The phytoclasts in the OBA D-8 well are dominated by translucent particles (55%–27%, 39.9% on average) as opposed to low to moderate amounts of opaque phytoclasts (7%–32%, 22.1% on average) (Figure 7). The OBA D-17 and OBA D-10 wells located slightly to the south of OBA D-8 display high concentrations of phytoclast particles that are in the range of 52%–90% (63.6% on average) and 52%–82% (66.9% on average), respectively (Figures 6 and 7). Opaque wood debris (20%–90%, 49% on average) dominate the phytoclast content in the OBA D-17 well versus a low concentration of translucent phytoclasts (14.6% on average) compared to the OBA D-10 well, which records moderate relative abundances of translucent (17%–57%, 36.9% on average) and opaque phytoclasts (15%–45%, 30.1% on average) (Figures 6 and 7). The AOM concentrations in the OBA D-17 and OBA D-10 wells are similar, in the range of 10%–40% (28.1% on average) and 10%–39% (24.7% on average) of the total POM composition. The phytoclast contents in the THAX-1 well record high values that are up to 85%

with an average of 71.9% of the total POM composition; they are dominated by translucent phytoclasts (41%–65%, 52.2% on average) versus low to moderate percentages of opaque phytoclasts (10%–35%, 19.7% on average). Low to moderate amounts of AOM (5%–31%, 18.9% on average) and palynomorph contents (2%–15%, 9.2% on average) are also reported in PFA-1 of the THAX-1 well.

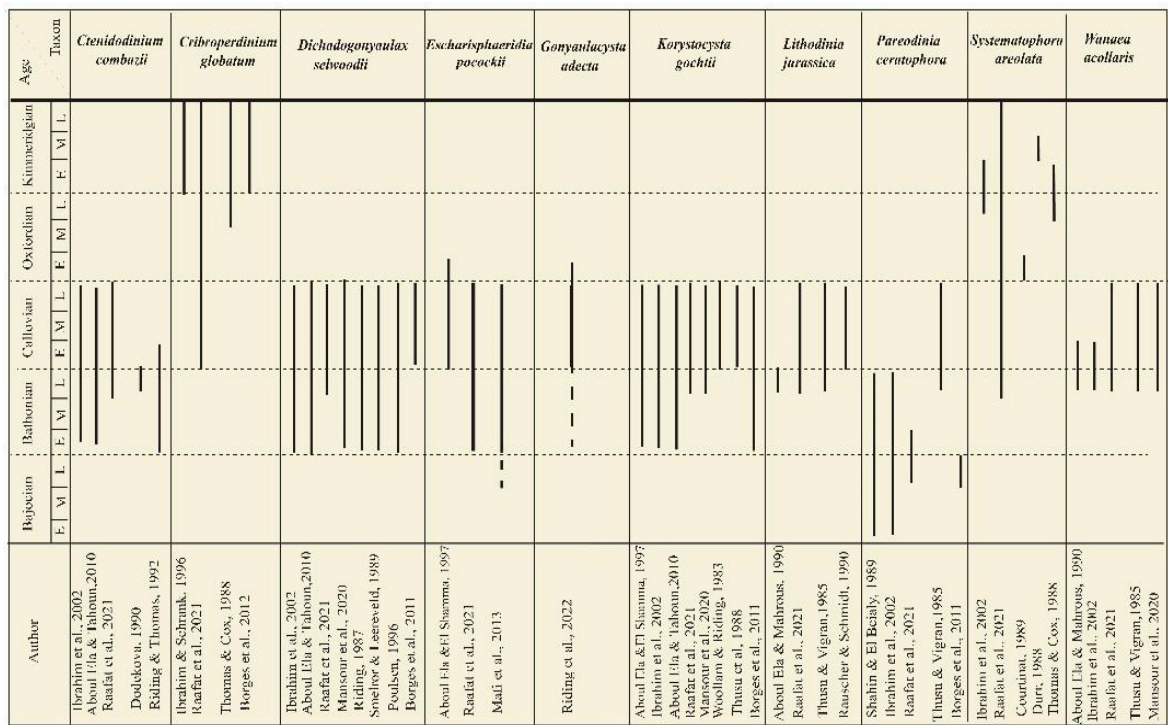


Figure 9. Distribution range chart of the most important age-diagnostic taxa recovered from the Khatatba Formation in the studied wells and their age ranges in comparison to published works of Ibrahim et al. [27], Aboul Ela & Tahoun [28], Dodekova [29], Riding et al. [30], Ibrahim & Schrank [31], Thomas & Cox [32], Borges et al. [33], Riding [34], Smelror & Leereveld [35], Poulsen [36], Borges et al. [37], Aboul Ela & El-Shamma [38], Mafi et al. [39], Riding et al. [40], Woollam & Riding [41], Thusu et al. [42], Aboul Ela & Mahrous [43], Thusu & Vigran [44], Rauscher & Schmitt [45], Shahin & El Beialy [46], Courtinat [47], Dürr [48].

PFA-2 occupies several intervals of the Khatatba Formation, and is represented by eight, seven, three, two, and two samples in the OBA D-10, THAX-1, OBA D-8, OBA D-17, and Falak-21 wells, respectively. All the PFA-2 samples plot in palynofacies field VI in the APP ternary diagram (Figure 8). PFA-2 is characterized by moderate relative abundances of phytoclasts and AOM contents and a minor contribution of the palynomorphs (Figure 5B,D). In the OBA D-10 well, the phytoclast and AOM contents are in the range of 45%–59% (51.8% on average) and 35%–50% (42.1% on average), respectively (Figure 7). The phytoclast contents have a higher concentration of opaque particles (20%–49%, 30.9% on average) compared to a slightly lower contribution of translucent phytoclasts (5%–30%, 20.9% on average). PFA-2 in the THAX-1 well exhibits similar contributions of both phytoclasts and AOM in that both are in the range of 42%–55% (47.3% on average) and 35%–53% (44.6% on average), respectively. The average palynomorph composition in the THAX-1 well is slightly higher (8.1%) than in the OBA D-10 well (6.1% of the total POM composition).

PFA-3 is represented by a few samples within the Khatatba Formation, and is comprised of six, two, two, and one samples in the THAX-1, OBA D-8, OBA D-17, and OBA D-10 wells, respectively (Figures 7 and 8). The PFA-3 samples plot in palynofacies fields IVa and IVb in the APP ternary diagram (Figure 8). In the THAX-1 well, PFA-3 is characterized by a moderate to high percentage of phytoclasts (44%–73%, 57.3% on average), low to mod-

erate AOM (11%–41%, 27.5% on average), and enhanced concentration of palynomorph grains (11%–17% of the total POM composition, 15.2% on average) (Figure 5C). The phytoclast contents are dominated by translucent phytoclasts (16%–54%, 36.8% on average), roughly twice the number of opaque phytoclasts (15%–28%, 20.5% on average) (Figure 7). The PFA-3 samples in the OBA D-8, OBA D-17, and OBA D-10 wells exhibit similar amounts of the three endmembers of phytoclasts, AOM, and palynomorphs (Figures 6 and 7) in comparison to the THAX-1 well.

PFA-4 is represented by eight samples, as follows: Falak-21 (two samples), OBA D-8 (three samples), OBA D-17 (two samples), and THAX-1 wells (one sample), all of which plot in palynofacies fields IX, VII, and VIII (Figure 8). PFA-4 is characterized by a high concentration of the AOM content compared to low to moderate percentages of phytoclasts and palynomorphs (Figure 5E). The highest amount of AOM content is recorded in the Falak-21 well (61.8%–74%) compared to the OBA D-8 well (49%–65%) (Figure 7). The phytoclasts in the Falak-21 and OBA D-8 wells are in the range of 23.6%–37% and 30%–39%, respectively (Figure 7). Similar POM compositions are reported in the OBA D-17 and THAX-1 wells (Figure 6).

5. Discussion

5.1. Age Assignment

In the Western Desert of Egypt, the Jurassic rock units are widespread and represented mainly by subsurface strata. The utilization of first downhole occurrence (FDO) in addition to the common occurrence (CO) is a good practice when working with cuttings, where caving while drilling is possible. Within the Khatatba Formation, relative age determination was reconstructed based on the FDO of biostratigraphic-significant marker dinoflagellate cyst taxa. They include *Adnatosphaeridium caulleryi*, *Dichadogonyaulax sellwoodii*, *Escharisphaeridia pocockii*, *Gonyaulacysta adecta*, *Korystocysta gochtii*, *Korystocysta pachyderma*, *Lithodinia jurassica*, *Pareodinia ceratophora*, and *Wanaea acollaris* (Figures 3 and 4). A schematic correlation of the FDO of the most important marker dinoflagellate cysts from the Middle Jurassic strata in Egypt and regionally from the European sections is shown in Figure 9.

In the upper part of the formation, the FDO of *Dichadogonyaulax sellwoodii* is commonly used as a marker dinoflagellate cyst of the Middle Jurassic (late Bathonian to Callovian) in northern Egypt [5,6,28,31,38,49,50]. Additionally, Gentzis et al. [4] documented the last appearance datum of *D. sellwoodii* within the lowermost part of the lower Oxfordian Masajid Formation, reinforcing an age not younger than Callovian. This index species was also utilized as a Bathonian to Callovian age indicator in the Boreal [34] and northwestern Tethys Realms [35]. In the Arctic Norway, Thusu [51] assumed an early-late Callovian age based on the marker *D. sellwoodii*, while Riding et al. [52] reported this index species from the type area of the Bathonian Stage in England. In the eastern Netherlands, a mid-late Callovian age was assigned based on the common occurrence of *D. sellwoodii* in the Achterhoek strata [53]. This is consistent with the common occurrence of *Korystocysta gochtii*, which is another age-diagnostic index species of the late Bathonian–Callovian in the north Western Desert [4–6,49,50,54] and Sinai [38]. Regionally, Borges et al. [37] reported *K. gochtii* from a Bathonian–Callovian palynostratigraphic zone in southern Portugal.

The CO of *Gonyaulacysta adecta* was utilized as a remarkable bioevent of the Middle Jurassic (Callovian) [40]. This species was recorded in the uppermost interval of the Khatatba Formation samples in the OBA D-10 well, supporting the proposed Middle Jurassic age of the studied succession (Figure 9). Another important record in this upper part of the Khatatba Formation is the occurrence of *Wanaea acollaris*, which was reported for the first time in the Bathonian sediments of Bulgaria [55]. The FDO of this marker dinoflagellate cyst defines an age no younger than late Callovian, as is the case in the Khatatba Formation in northern Egypt [38,50], the upper Bathonian–Callovian sediments in northeast Libya [42], and the upper Bathonian–Callovian strata in southern France [35] and Spain [56]. Other age-diagnostic marker taxa, such as *Lithodinia jurassica*, *Adnatosphaeridium caulleryi*, and *Escharisphaeridia pocockii*, have been commonly recorded in the upper Bathonian–Callovian

strata of the Khatatba Formation in Egypt [5,6,50]. Regionally, these marker species were reported in the late Bathonian–Callovian in northeast Libya [42], the early Callovian in Lincolnshire, England [34], and the mid-Bathonian to Callovian in northeast Spain and Portugal [56]. The dinoflagellate cyst *Cribroperdinium globatum* is commonly reported in the Upper Jurassic (Kimmeridgian) sediments of the Algarve Basin in Portugal, but the first appearance or basal occurrence could support a Middle Jurassic age [37]. In this study, it is rarely recorded in the upper parts of the Khatatba Formation in the OBA D-10 and THAX-1 wells, except for the uppermost two samples in the OBA D-8 well that contained slightly higher contents of 6% on average of total palynomorph composition (Table S1), indicating a Middle Jurassic age of the studied samples. The chorate genus *Systematophora* and related species recorded in the upper part of the Khatatba Formation, which is mostly represented by *Systematophora* sp. (Table S1). The CO of *Systematophora areolata* took place during the middle–late Oxfordian to early Kimmeridgian of England [30,32] and southern Portugal [37]. However, Borges et al. [37] and Prauss [57] noticed the occasional reports of *Systematophora areolata* in the Bathonian and Callovian sediments, respectively, which are consistent with the current study records of this species in the Middle Jurassic Khatatba Formation. Similarly, the CO of *Systematophora penicillata* was reported from the Kimmeridgian strata in Germany [48] and England [30]. In Egypt, it was recorded from the Middle Jurassic (Bathonian–Callovian) strata in the north Western Desert [50] and from the Callovian–Oxfordian sediments in Sinai [58]. Occasional records of *Systematophora penicillata* in the upper part of the Khatatba Formation reinforce a Middle Jurassic (Bathonian–Callovian) age.

The lower part of the Khatatba Formation is assigned to the upper Bajocian to lower Bathonian based on the abundant occurrence of the index taxon *Pareodinia ceratophora* in the OBA D-8, OBA D-10, OBA D-17, and THAX-1 wells. Although *P. ceratophora* is commonly recorded in the Bathonian–Callovian worldwide [33], it may occur sporadically in the Late Jurassic [59]. It has been recorded in the Bajocian strata of Lincolnshire in England [34] and the early Bajocian–Callovian in the northern part of the North Sea [60]. Keeley et al. [8] reported it as a marker species in the Bajocian–Bathonian strata in the north Western Desert. Furthermore, its occurrence can be correlated with the Bajocian *Pareodinia ceratophora* Interval Zone in northwest Germany [57]. Detailed palynostratigraphic zones and age assignments of the OBA D-8 and OBA D-10 wells are available in Raafat et al. [6].

5.2. Palynofacies Analysis and Kerogen Characterization

The analogous stratigraphic variations in the POM composition include changes in AOM, translucent and opaque phytoclasts, various terrestrial (plant spores and pollen grains) and marine palynomorph groups (chorate, proximate, and proximochorate dinoflagellate cysts and MFTLs), and the M:T ratio. These palynofacies proxies are implemented as reliable tools to interpret characteristics of kerogen types and compositions and trace the changes in relative sea level and the proximity trends of shorelines [12,13,61–67]. Based on the major distribution of samples in the APP ternary plot of Tyson [12] along with the stratigraphic variation in POM composition, four palynofacies assemblages were inferred (see Section 4.2; Figure 8).

PFA-1 is dominant throughout the Khatatba Formation in the five wells (75 samples), especially in the middle and lower intervals of the formation. It is characterized by a relatively high abundance of phytoclasts compared to low relative abundances of AOM and palynomorphs (Figures 6 and 7). All the PFA-1 samples plot in palynofacies field II on the APP ternary diagram (Figures 5A and 8). The preserved organic matter is mainly kerogen Type III and a likely source for gas-prone hydrocarbons. Excess input of terrigenous organic matter in shallow marine shelf and marginal marine areas can trigger significantly high values of total phytoclast contents (80% on average) [12,13]. Rock-Eval HI is commonly used to reveal the type of kerogen. The visual assessment of the PFA-1 kerogen type is consistent with organic geochemical measurements of the Khatatba Formation in the

region, mostly in the Shushan Basin, as noted below. Geochemical characterization of the formation in the Lotus-1 well in the western part of the Shushan Basin recorded relatively low HI values that are in the range of 100–200 mg HC/g TOC, indicating Type III kerogen of gas-prone potential [10]. Shalaby et al. [11] reported that most of the Khatatba Formation samples in the Shams and Tut gas fields were dominated by terrestrial organic matter of kerogen Type III based on the HI values (63–198 mg HC/g TOC). This is consistent with similar results from 18 wells studied by El Diasty et al. [9] in the Shushan Basin, where the majority of the samples recorded HI values between 100 and 200 mg HC/g TOC. Additionally, Mansour et al. [5] indicated that the Khatatba Formation in the Falak-21 well was dominated by low to moderate HI values (63–190 mg HC/g TOC) and inferred a humic organic matter typical of gas-prone Type III kerogen.

PFA-2 is sporadically recorded at some intervals of the Khatatba Formation in the studied wells (Figures 6 and 7). PFA-2 is dominated by moderate relative abundances between the phytoclast content and AOM (Figures 5B and 8). According to the APP ternary plot of Tyson [12], the samples plot in palynofacies field VI, which is characterized by Type II kerogen with oil-prone potential. This inference can be supported by the aforementioned studies in the Shushan Basin. For example, Alsharhan and Abd El-Gawad [10] measured moderate HI values (240 mg HC/g TOC) for a mixed kerogen Type II/III in the upper part of the Khatatba Formation in the JB26-1 well. Moderate HI values (106–261 mg HC/g TOC, average of 191 mg HC/g TOC) were reported in the Shams NE-1 well, where the type of kerogen varies between Type III and mixed Type II/III [11]. El Diasty et al. [9] indicated that few samples from the Khatatba Formation reached >200 mg HC/g TOC, suggesting mixed organic matter of Type II/III kerogen.

Phytoclast-palynomorph-dominated PFA-3 occurs in 11 sampling intervals within the Khatatba Formation in four wells, excluding Falak-21. Consisting mainly of total phytoclasts that reach up to 73% with some contribution of different palynomorph categories (up to 17% of the total POM composition) (Figures 6 and 7), all the samples plot in palynofacies fields IVa and IVb. While both fields are characterized by abundant occurrences of palynomorph groups, field IVa has a slightly higher contribution of total phytoclast content than field IVb, the latter of which has moderate relative abundances between the AOM and phytoclasts. POM composition of both fields IVa and IVb indicates that the preserved organic matter is kerogen Type III with gas-prone potential. The inferred kerogen type of these fields is consistent with the aforementioned HI values from the Shushan Basin [5,9–11].

PFA-4 is sparsely recorded in eight samples in four wells, except for OBA D-10 (Figures 6 and 7). It is an AOM-dominated assemblage, and all the samples plot in palynofacies fields VII, VIII, and IX (Figures 5D and 8). The AOM content reached to 74% of the total POM composition in the Falak-21 well compared to the relatively low percentages of the total phytoclast contents. The three palynofacies fields denote excess AOM of oil-prone kerogen Type II. However, none of the available studies of the Khatatba Formation in this region of the north Western Desert recorded high HI values that inferred Type II kerogen of oil-prone potential.

Comparing the optical palynofacies assessment of the types of kerogen versus organic geochemistry based on Rock-Eval HI values has provided reliable inferences for the major characterization of preserved organic matter. Of note, PFA-1 and PFA-3 results are consistent with HI values for the Khatatba Formation. PFA-2 and PFA-4 are dominated by moderate to high percentages of AOM, respectively, and reveal oil-prone Type II kerogen.

5.3. Paleoenvironmental Reconstruction

Palynomorph composition and palynofacies analysis of preserved POM are important tools in paleoenvironmental reconstructions as well as for optimal exploration of hydrocarbon source and reservoir intervals [67]. The compositions of the recovered organic matter, palynomorph groups, and M:T ratio within the Khatatba Formation provide a good opportunity to discriminate between diverse depositional settings. The M:T ratio is an important palynological proxy that reveals the phases of relative sea level change and thus a change

in the depositional environment [5,66,68]. Generally, a low M:T ratio (below 1) points to a phase of relative sea level fall and a shallowing of the prevalent environmental setting, whereas a high M:T ratio (above 1) indicates a gradual transgression of relative sea level and, therefore, a deepening of the depositional environment.

5.3.1. PFA-1

The predominance of phytoclasts in the 75 PFA-1 samples (Figure 5A) in palynofacies field II (Figure 8) indicates their deposition in marginal dysoxic–anoxic basin conditions [12]. In the Falak-21 well, the phytoclasts are dominated by opaque equidimensional phytoclasts that average 76.2% versus translucent phytoclasts (average 3%) (Figure 7), suggesting nearby active fluvio-deltaic source areas [13]. Increased opaque phytoclasts in such settings indicate significant oxidation of terrestrial phytoclast particles, likely under active littoral conditions, whereby tidal activity and consequent oscillations of the water table are the main controlling processes [12]. This agrees with the lithofacies of the Khatatba Formation, which consist of intercalations between fine siltstones and sandstones (Figure 7). Additionally, the very low M:T ratio (0.3 on average) of PFA-1 in the Falak-21 well suggests a high terrestrial influx likely during a phase of sea level lowstand [13,63,66]. Abundant occurrences of plant spores versus low proportions of dinoflagellate cysts indicate a proximal setting close to an active fluvio-deltaic source, especially for thick-walled and ornamented spores that indicate a short distance of POM transport [13,26,63]. In the Falak-21 well, moderate to high contents of spores (up to 86.4%, 44.8% on average) and pollen grains (up to 57.9%, 35.5% on average) are reported compared to low average values of dinoflagellate cysts (up to 50% of total palynomorph composition, 17.1% on average). This palynomorph composition implies a short distance of transportation and deposition of the PFA-1 samples close to an active fluvio-deltaic setting [13]. This interpretation is supported by the prevalent abundance of the psilate spore *Cyathidites* and *Deltoidospora* groups along with thick-walled *Gleicheniidites* and ornamented *Microreticulatisporites* (Figure 5).

Within the Khatatba Formation in the THAX-1 well, translucent phytoclasts dominate (up to 65%, 52.2% on average) versus opaque phytoclasts (up to 35%, 19.7% on average) (Figure 8), suggesting the accumulation of phytoclasts after a short distance of transportation and deposition in a proximal environment near an active fluvio-deltaic source [12,13]. However, enhanced oxidation and/or thermal alteration of part of the translucent phytoclasts cannot be excluded, especially since the formation is currently in the oil window of organic matter maturation [5,6]. Additionally, the palynomorph composition in this well is dominated mainly by terrestrial palynomorphs, mostly spores (up to 62%, 44.1% on average) and pollen grains (up to 50%, 24.8% on average) compared to diminished proportions of dinoflagellate cysts (27.8% on average) (Figure 6). The spore content is dominated by an overabundance of *Deltoidospora* and *Gleicheniidites* groups, reinforcing a proximity to a fluvio-deltaic setting and deposition during warm humid climates [13]. In addition, the M:T ratio is significantly low (0.1–1, 0.5 on average) in the THAX-1 well. Thus, enhanced contributions of spores and pollen grains versus reduced proportions of dinoflagellate cysts support the deposition in a marginal shallow marine environment and proximity to an active fluvio-deltaic source area [12,13]. This is consistent with the occurrence of acritarchs (up to 11%, 3.3% on average), which infers deposition in a marginal brackish water depositional environment [13,69,70].

The dominance of phytoclasts in the PFA-1 samples in the OBA D-8, OBA D-10, and OBA D-17 wells (Figures 6 and 7) suggests deposition in close proximity to active fluvio-deltaic environments [13]. However, unlike the Falak-21 well, the OBA D-8 and OBA D-10 wells preserve moderate relative abundances of the translucent and opaque phytoclasts (Figures 6 and 7), with translucent phytoclasts reaching up to 55% (40% on average) and 57% (37% on average), respectively, compared to opaque phytoclasts with up to 32% (22.1% on average) and 45% (30.1% on average), respectively. The higher concentrations of the translucent phytoclasts relative to opaque fragments reveal a shallowing upward setting that was gradually introduced into more proximal conditions close to fluvio-deltaic

source areas [5,6,12,13,66,67]. Furthermore, the proportions of opaque phytoclasts in both wells infer significant oxidation of the translucent plant fragments after a long distance of riverine transport and accumulation in shallow marine settings not far from the shore. In contrast, the palynofacies characteristics in the OBA D-17 well are similar to those in the Falak-21 well. The higher proportion of opaque phytoclasts (49% on average) compared to translucent wood particles (14.6% on average) (Figure 6) reinforces the significant oxidation of translucent phytoclasts after a long distance of POM transport [13,62].

It appears that while the PFA-1 samples in the OBA D-8, OBA D-10, and OBA D-17 wells infer deposition near fluvio-deltaic sources, they were located in slightly distal shallow marine shelf conditions compared to the Falak-21 and THAX-1 wells. This interpretation is supported by the highest concentrations of dinoflagellate cysts within the Khatatba Formation in the OBA D-8, OBA D-10, and OBA D-17 wells with average values of 99.7%, 64.6%, and 88% of total palynomorph composition, respectively, compared to the significantly lower average values of 17.1% in the Falak-21 well [5]. Increased relative abundances of dinoflagellate cysts indicate deposition in areas of high dinoflagellate marine productivity, such as a shelf-front depositional setting [15,71,72]. In OBA D-8, the dinoflagellate proximate cysts *Sentusidinium*, *Escharisphaeridia*, and *Dissiliodinium* dominate; these forms occur abundantly in coastal to marginal shallow marine shelf environments [5,50]. In the OBA D-10 and OBA D-17 wells, the dinoflagellate cysts are represented by the aforementioned proximate groups along with common occurrences of *Korystocysta*, *Dichadogonyaulax*, and the chorate *Systematophora* groups. *Korystocysta* and *Dichadogonyaulax* are mainly restricted to shallow marine shelf settings [52], while *Systematophora* dominates in slightly deeper shelf conditions [66]. Additionally, the absence of spores in the OBA D-8 well and their low proportions in the OBA D-10 (19.3% on average) and OBA D-17 wells (3.4% on average) compared to Falak-21 (44.8%) indicate a slightly deeper water column in shallow shelf environmental conditions where the three OBA D wells are located [67]. Our results are consistent with enhanced M:T ratios in the OBA D-10 (8.1–0.8, 2.3 on average) and OBA D-17 wells (13.3–0, 4.4 on average) (Figures 6 and 7).

5.3.2. PFA-2

The 22 PFA-2 samples in the five studied wells, represented mostly in the OBA D-10 and THAX-1 wells, usually occur in the upper intervals of the Khatatba Formation and are dominated by moderate proportions between phytoclasts and AOM with some palynomorphs (Figure 5B,D). With these samples plotting in palynofacies field VI due to significant contributions of terrestrial and marine organic matter, deposition in a proximal suboxic to anoxic inner shelf environment is inferred that is deeper in comparison to PFA-1 [12,13]. This is consistent with the intercalations of limestones and shales in the Upper Safa and Zahra rock units in the upper part of the Khatatba Formation (Figures 6 and 7). Despite the phytoclast content showing a gradual upward decrease in the uppermost part of the OBA D-10 well relative to a gradual increase in AOM, the average values of phytoclasts (51.8%) are higher than AOM (42.1%) (Figure 7). The AOM and total phytoclast contents are similar, with average values of 44.6% and 47.3%, respectively, in the THAX-1 well. The enhanced AOM content indicates deposition under a relatively low-energy, oxygen-deprived aquatic setting that triggered potential preservation of organic matter [5,13,63]. This interpretation is consistent with the higher average contribution of opaque phytoclasts (30.9%) compared to translucent wood particles (20.9%) in the OBA D-10 well, indicating a long transport distance of POM via terrestrial/riverine input in shallow shelf settings. In contrast, the total phytoclast contents in the THAX-1 well are dominated by translucent phytoclasts compared to diminished opaque phytoclasts with average values of 30.7% and 16.6%, respectively, suggesting close proximity to active riverine sources and deposition in a slightly shallower setting than the OBA D-10 well.

The dinoflagellate cyst content in the OBA D-10 well (up to 80.3%), with an average of 51.8% of total palynomorph composition compared to spores and pollen grains with average values of 31.5% and 16.6% (Figure 7), respectively, reveals deposition in an

inner neritic shelf environment [13,66,71,72]. This is in agreement with the moderate to high M:T ratios that reach up to 4.1 (1.6 on average). The dinoflagellate cysts are dominated by abundant occurrences of the *Systematophora*, *Korystocysta*, and *Dichadogonyaulax* groups, with some records of the chorate *Oligosphaeridium* sp., while the proximate forms *Sentusidinium* and *Escharisphaeridia* decreased significantly and *Dissiliodinium* was absent compared to their abundant occurrences in PFA-1. The abundance of *Oligosphaeridium* sp. infers a distal outer neritic shelf to open oceanic conditions [71–73]; therefore, its record along with *Systematophora* and other dinoflagellate taxa reveal deposition in proximal inner neritic shelf conditions. The spore content is dominated mainly by *Deltoidospora* sp. And *Deltoidospora minor* with sparse records of *Gleicheniidites* spp., while the pollen grain content is characterized by prevalent abundances of sphaeromorph forms, including *Inaperturopollenites* sp. And *Spheripollenites psilatus*. These terrestrial palynomorphs reinforce deposition in a more distal part of an inner shelf environment compared to PFA-1 [13].

The palynomorph composition in the THAX-1 well is characterized by the high abundance of spores with an average of 59% compared to dinoflagellate cysts (28.9%) and pollen grains (12.1%) (Figure 6), suggesting deposition in a shallower shelf setting than the OBA D-10 well. This is consistent with the significantly low M:T ratios (0.6 on average) in this well. Unlike the OBA D-10 well, the chorate *Oligosphaeridium* sp. is absent in the THAX-1 well, while *Systematophora* is sparsely recorded. The dinoflagellate cysts are mostly represented by *Sentusidinium*, *Dichadogonyaulax*, and *Korystocysta*, which are more restricted to coastal and proximal inner shelf environments [50,52,66]. The spore content is dominated mainly by the *Deltoidospora* (up to 56% of total palynomorph composition) and *Gleicheniidites* groups (up to 16.2%), with sparse records of the *Concavisporites* group, reinforcing deposition in proximal inner shelf settings not far from the shore [13,66].

5.3.3. PFA-3

PFA-3 occupies minor intervals that intercalate consistently with PFA-1 within the Khatatba Formation and is represented by 11 samples in four of the studied wells. It is characterized by moderate to high average values of the terrestrial phytoclasts compared to the low to moderate proportions of the AOM and palynomorphs (Figure 5C), and plot in palynofacies fields IVa and IVb (Figure 8). Both palynofacies fields indicate the deposition in a shelf-to-basin transition with respect to increasing basin subsidence and/or water column depth [12,13]. Specifically, field IVa indicates deposition under enhanced dysoxic to suboxic redox conditions, whereas field IVb reflects more severe redox conditions and deposition under a suboxic to anoxic water column setting [13]. Of note, the PFA-3 samples that plot in field IVb have significantly higher proportions of AOM (40.3% on average) compared to those in field IVa (17.8% on average) (Figures 6 and 7). This indicates that samples that plotted in palynofacies field IVB were deposited in a relatively distal, low-energy, oxygen-depleted setting compared to samples in field IVa [5,13,63]. This is consistent with the palynomorph composition, which is characterized by high average values of dinoflagellate cysts in OBA D-8 (100%), OBA D-17 (87.5%), and OBA D-10 (69%), compared to low occurrences or the absence of spores and pollen grains (Figures 6 and 7). The moderate to high average values of the M:T ratio in the OBA D-17 (7.3) and OBA D-10 wells (2.2) along with palynomorph characteristics underpin the deposition of the PFA-3 samples in deeper conditions, such as a distal inner neritic shelf setting. This is because dinoflagellate cysts are dominated by shallow marine shelf proximate forms, including *Sentusidinium* spp., *Escharisphaeridia* sp., and *Dissiliodinium* sp., with low records or absence of the chorate forms *Oligosphaeridium* sp. and *Systematophora* sp. In the THAX-1 well, deposition appears to be under a proximal inner neritic shelf setting compared to the OBA D wells due principally to the higher average proportions of spores (59%) in comparison to dinoflagellate cysts (28.9%) and pollen grains (12.1%). These palynomorph characteristics accounted for the significantly low average values of the M:T ratios of 0.4 compared to the higher values in the OBA D wells. The spore content is characterized by a prevalent abundance of *Deltoidospora* (up to 59.5%) and *Gleicheniidites* groups (up to 10.5% of total

palynomorph composition), reinforcing the interpretation of a slightly proximal setting compared to the OBA D wells [13,66]. In addition, the dinoflagellate cysts are comprised of *Sentusidinium* spp., *Escharisphaeridia* sp., *Dichadogonyaulax* sp., and *Ctenidodinium* spp., with rare occurrences of *Systematophora* sp., reinforcing deposition in a proximal inner neritic shelf environment [52,71,72].

5.3.4. PFA-4

The eight PFA-4 samples in four of the studied wells are characterized by moderate to high proportions of the AOM compared to the low to moderate relative abundances of terrestrial phytoclasts and palynomorphs (Figure 5E) and plot in palynofacies fields IX, VII, and VIII (Figure 8). Field IX indicates the deposition of samples in a distal suboxic to anoxic basin under a stratified water column setting, whereas fields VII and VIII reflect the deposition under a distal dysoxic to anoxic shelf with enhanced organic matter preservation typical of organic carbon-rich accumulations [12,13]. High to moderate AOM proportions, along with frequent occurrences of small pyrite inclusions within the AOM in the Falak-21 and OBA D-8 wells, reveal accumulation of fine sediments under low-energy, well-stratified, oxygen-depleted water column settings (Figure 7) [13,63]. Further evidence from the total sulfur and total organic carbon values from the Falak-21 well attested to the predominant deposition of the upper part of the Khatatba Formation under enhanced suboxic conditions [5]. Additionally, the palynomorph composition is characterized by high values of dinoflagellate cysts with some records of the MFTLs compared to few pollen grains and few to no spores in the Falak-21, OBA D-8, and OBA D-17 wells. These are consistent with high M:T ratios with average values of 1.1, 17.8, and 6.2 in the Falak-21, OBA D-8, and OBA D-17 wells, respectively (Figures 6 and 7). The dinoflagellate cysts in the above three wells are comprised of a mixture of proximate and chorate forms, including *Cribroperidinium* spp., *Dichadogonyaulax sellwoodii*, *Escharisphaeridia pocokii*, *Lithodinia jurassica*, *Korystocysta* spp., *Sentusidinium* spp., and *Systematophora* sp., which reinforces deposition in a distal inner neritic basin [52,66,71,72].

To sum up, the preserved POM and related palynofacies and palynomorph proxies indicate that PFA-1 of the Khatatba Formation was deposited near an active fluvio-deltaic setting in a marginal shallow marine environment. However, sediments of the three OBA D wells appear to have been deposited in a slightly distal setting compared to those of the more proximal THAX-1 and Falak-21 wells (Figures 6 and 7). Moderate relative abundances between AOM and phytoclasts represent the POM of PFA-2, which was recovered in 22 samples mostly in the OBA D-10 and THAX-1 wells, indicating the deposition in a proximal suboxic to anoxic relatively low-energy inner shelf environment. Abundant chorate dinoflagellate cysts along with sphaeromorph pollen support the deposition of PFA-2 in a more distal part of an inner shelf setting compared to PFA-1. PFA-3 is comprised of moderate to high proportions of the terrestrial phytoclasts versus the low to moderate average values of the AOM and palynomorphs, revealing deposition in a proximal inner neritic shelf-to-basin transition under enhanced oxygen-deprived dysoxic to anoxic redox conditions. In contrast, PFA-4 is dominated by moderate to high AOM versus low phytoclasts and moderate to low palynomorphs, suggesting deposition under an enhanced suboxic to anoxic well-stratified distal inner neritic shelf environment.

6. Conclusions

The Middle Jurassic Khatatba Formation, which is the principal source rock interval in the north Western Desert, is investigated in this study following an approach of palynomorph and palynofacies analyses in five wells in the Matruh, Shushan, and Dahab-Mireir Basins to assess the depositional age, kerogen characteristics, and reconstruct depositional paleoenvironmental settings. The palynomorph composition indicates a rich assemblage of moderately diverse plant spores, pollen grains, and dinoflagellate cysts. Based on the first downhole occurrence of age-diagnostic dinoflagellate cyst taxa, a Bajocian to Callovian age was assigned to the Khatatba Formation. This includes the FDO of the marker taxa

Dichadogonyaulax sellwoodii, *Korystocysta gochtii*, *Lithodinia jurassica*, *Pareodinia ceratophora*, and *Wanaea acollaris*. The palynofacies analysis revealed four assemblages, as follows: PFA-1 is phytoclast-dominated and gas-prone kerogen Type III; PFA-2 is phytoclast-AOM-dominated and oil-prone kerogen Type II; PFA-3 is phytoclast-AOM-dominated with enhanced palynomorph composition and gas-prone kerogen Type III; and PFA-4 is AOM-dominated and oil-prone kerogen Type II. Based on the major characteristics of the four palynofacies assemblages and palynomorph compositions, detailed paleoenvironmental reconstructions were conducted. PFA-1 was deposited near active fluvio-deltaic sources to marginal marine conditions, whereas PFA-2 and PFA-3 were deposited under enhanced dysoxic–suboxic and suboxic–anoxic proximal inner neritic shelf environments, respectively. PFA-4 was deposited under a prevalent suboxic–anoxic distal inner neritic basin due to abundant proportions of AOM and proximate dinoflagellate cysts and some chorate forms. These results reveal that the Middle Jurassic was a time of marginal to shallow marine environment in this part of the southern margin of the Tethys, where the north Western Desert was located. Further future palynological and palynofacies investigations of the important Khatatba Formation in northern Egypt are highly recommended.

Supplementary Materials: The following supporting information can be downloaded at: <https://www.mdpi.com/article/10.3390/min13040548/s1>, Figure S1: Palynofacies (kerogen) groups; Table S1: Palynomorph assemblage; Table S2: Concentrations of phytoclasts and palynomorphs.

Author Contributions: Conceptualization, A.M. and S.S.T.; methodology, A.M. and A.R.; software, A.M. and A.R.; validation, A.M., S.S.T., T.G., F.O.-I., M.S.A. and X.F.; formal analysis, A.M.; investigation, A.M. and A.R.; resources, A.M. and A.R.; data curation, F.O.-I. and M.S.A.; writing—original draft preparation, A.M.; writing—review and editing, A.M., F.O.-I. and T.G.; visualization, A.R.; supervision, F.O.-I. and X.F.; project administration, A.M.; funding acquisition, M.S.A. All authors have read and agreed to the published version of the manuscript.

Funding: This work was funded by Researchers Supporting project number (RSP2023R455), King Saud University, Riyadh, Saudi Arabia.

Data Availability Statement: Data is contained within the article or supplementary material.

Acknowledgments: We thank the Egyptian General Petroleum Corporation, Badr El Din Petroleum Company, and the Agiba Petroleum Company in Cairo, Egypt, for their permissions to obtain cutting rock samples and composite logs of the five wells. The authors would like to thank editor Alexandru Gabriel Calin for his professional handling of the manuscript and the two anonymous reviewers whose comments and suggestions improved the quality of the manuscript.

Conflicts of Interest: The authors declare no conflict of interest.

References

1. Haq, B.U. Jurassic Sea-Level Variations: A Reappraisal: The Geological Society of America Today. *GSA Today* **2018**, *28*, 4–10. [[CrossRef](#)]
2. EGPC (Egyptian General Petroleum Corporation). *Western Desert, Oil and Gas Fields (A Comprehensive Overview)*; EGPC: Cairo, Egypt, 1992; p. 431.
3. Abrams, M.A.; Greb, M.D.; Collister, J.W.; Thompson, M. Egypt far Western Desert basins petroleum charge system as defined by oil chemistry and unmixing analysis. *Mar. Pet. Geol.* **2016**, *77*, 54–74. [[CrossRef](#)]
4. Gentzis, T.; Carvajal-Ortiz, H.; Deaf, A.S.; Tahoun, S.S. Multi-proxy approach to screen the hydrocarbon potential of the Jurassic succession in the Matruh Basin, North Western Desert, Egypt. *Int. J. Coal Geol.* **2018**, *190*, 29–41. [[CrossRef](#)]
5. Mansour, A.; Geršlová, E.; Sýkorová, I.; Vöröš, D. Hydrocarbon potential and depositional paleoenvironment of a Middle Jurassic succession in the Falak-21 well, Shushan Basin, Egypt: Integrated palynological, geochemical and organic petrographic approach. *Int. J. Coal Geol.* **2020**, *219*, 103374. [[CrossRef](#)]
6. Raafat, A.; Tahoun, S.S.; Aboul Ela, N.M. Palynomorph biostratigraphy palynofacies thermal maturity and paleoenvironmental interpretation of the Bajocian-Aptian succession in the OBA D-8 Well Matruh Basin Egypt. *J. Afr. Earth Sci.* **2021**, *177*, 104157. [[CrossRef](#)]
7. Hantar, G. North Western Desert. In *The Geology of Egypt*; Said, R., Ed.; Chapter 15; Balkema: Rotterdam, The Netherlands, 1990; pp. 293–320.
8. Keeley, M.L.; Dungworth, G.; Floyd, C.S.; Forbes, G.A.; King, C.; McGarva, R.M.; Shaw, D. The Jurassic System in northern Egypt: I. Regional stratigraphy and implications for hydrocarbon prospectivity. *J. Pet. Geol.* **1990**, *13*, 397–420. [[CrossRef](#)]

9. El Diasty, W.S.; El Beialy, S.Y.; Littke, R.; Farag, F.A. Source rock evaluation and nature of hydrocarbons in the Khalda Concession, Shushan Basin, Egypt's Western Desert. *Int. J. Coal Geol.* **2016**, *162*, 45–60. [[CrossRef](#)]
10. Alsharhan, A.S.; Abd El-Gawad, E.A. Geochemical characterization of potential Jurassic/Cretaceous source rocks in the Shushan Basin, northern Western Desert, Egypt. *J. Pet. Geol.* **2008**, *31*, 191–212. [[CrossRef](#)]
11. Shalaby, M.R.; Hakimi, M.H.; Abdullah, W.H. Organic geochemical characteristics and interpreted depositional environment of the Khatatba Formation, northern Western Desert, Egypt. *Am. Assoc. Pet. Geol. Bull.* **2012**, *96*, 2019–2036. [[CrossRef](#)]
12. Tyson, R.V. Palynofacies Analysis. In *Applied Micropaleontology*; Jenkins, D.G., Ed.; Kluwer Academic Publications: Dordrecht, The Netherlands, 1993; pp. 153–191.
13. Tyson, R.V. *Sedimentary Organic Matter—Organic Facies and Palynofacies*; Chapman and Hall: London, UK, 1995; 615p.
14. Guiraud, R. Mesozoic rifting and basin inversion along the northern African Tetyan margin: An overview. In *Petroleum Geology of North Africa*; Macgregor, D.S., Moody, R.T.J., Clark-Lowes, D.D., Eds.; Geological Society: London, UK, 1998; pp. 217–229.
15. Keeley, M.L. Phanerozoic evolution of the basins of Northern Egypt and adjacent areas. *Geol. Rundschau* **1994**, *83*, 728–742. [[CrossRef](#)]
16. Guiraud, R.; Bosworth, W. Phanerozoic geodynamic evolution of northeastern Africa and the northwestern Arabian platform. *Tectonophysics* **1999**, *315*, 73–108. [[CrossRef](#)]
17. Said, R. Cretaceous Paleogeographic Maps. In *The Geology of Egypt*; Said, R., Ed.; Balkema: Rotterdam, The Netherlands, 1990; pp. 439–449.
18. Stampfli, G.M.; Mosar, J.; Favre, P.; Pillecuit, A.; Vannay, J.C. Permo-Mesozoic evolution of the western Tethys realm: The Neo-Tethys east Mediterranean basin connection. In *Peri-Tethys Memoir 6: Peri-Tethyan Rift/Wrench Basins and Passive Margins*; Ziegler, P.A., Cavazza, W., Robertson, A.H.F., Crasquin-Soleau, S., Eds.; Mémoires du Muséum National D'Histoire Naturelle de Paris; Muséum National D'Histoire Naturelle: Paris, France, 2001; Volume 186, pp. 51–108.
19. Bumby, A.J.; Guiraud, R. The geodynamic setting of the Phanerozoic basins of Africa. *J. Afr. Earth Sci.* **2005**, *43*, 1–12. [[CrossRef](#)]
20. Kerdany, M.T.; Cherif, O.H. Mesozoic. In *The Geology of Egypt*; Said, R., Ed.; Balkema: Rotterdam, The Netherlands, 1990; pp. 407–437.
21. Guiraud, R.; Bosworth, W. Senonian basin inversion and rejuvenated of rifting in Africa and Arabia: Synthesis and implications to plate-scale tectonics. *Tectonophysics* **1997**, *282*, 39–82. [[CrossRef](#)]
22. Moustafa, A.R. Mesozoic-Cenozoic basin evolution in the northern western desert of Egypt. *Geol. East Libya* **2008**, *2008*, 29–46.
23. Bevan, T.G.; Moustafa, A.R. Inverted rift-basins of northern Egypt: Phanerozoic rift systems and sedimentary basins. In *Regional Geology and Tectonics*; Roberts, D., Bally, A., Eds.; Section 4; Elsevier: Amsterdam, The Netherlands, 2012; Volume 2, pp. 483–506.
24. Bosworth, W.; El-Hawat, A.S.; Helgeson, D.E.; Burke, K. Cyrenaican “shock absorber” and associated inversion strain shadow in the collision zone of northeast Africa. *Geology* **2008**, *36*, 695–698. [[CrossRef](#)]
25. Norton, P. Rock Stratigraphic Nomenclature of the Western Desert. *Egypt. Int. Rep. GPC Cairo Egypt* **1967**, *557*, 18.
26. Traverse, A. *Paleopalynology*, 2nd ed.; Springer: Berlin/Heidelberg, Germany, 2007; p. 813.
27. Ibrahim, M.I.A.; Aboul Ela, N.M.; Kholeif, S.E. Dinoflagellate cyst biostratigraphy of Jurassic-Lower Cretaceous formations of the North Eastern Desert, Egypt. *Neues Jahrb. Für Geol. Und Paläontologie Abh.* **2002**, *224*, 255–319. [[CrossRef](#)]
28. Aboul Ela, N.M.; Tahoun, S.S. Dinoflagellate cyst stratigraphy of the subsurface Middle-Upper Jurassic/Lower Cretaceous sequence in North Sinai, Egypt. In Proceedings of the 5th International Conference on the Geology of the Tethys Realm, South Valley University, Qena, Egypt, 4–7 January 2010; pp. 85–115.
29. Dodekova, L. Dinoflagellate cysts from the Bathonian-Tithonian (Jurassic) of north Bulgaria. 1. Taxonomy of Bathonian and Callovian dinoflagellate cysts. *Geol. Balc.* **1990**, *20*, 3–45.
30. Riding, J.B.; Thomas, J.E. Dinoflagellate cysts of the Jurassic System. In *A Stratigraphic Index of Dinoflagellate Cysts*; Powell, A.J., Ed.; Chapman and Hall: London, UK, 1992; pp. 7–97.
31. Ibrahim, M.I.A.; Schrank, E. Palynological studies on the late Jurassic- early Cretaceous of the Kahraman-1 well, northern Western Desert, Egypt. In *Géologie de l'Afrique et de l'Atlantique Sud: Actes Colloques Angers*; 1996; pp. 611–629. Available online: <https://pascal-francis.inist.fr/vibad/index.php?action=getRecordDetail&idt=6263263> (accessed on 7 March 2023).
32. Thomas, J.E.; Cox, B.M. The Oxfordian-Kimmeridgian Stage boundary (Upper Jurassic): Dinoflagellate cyst assemblages from the Harome Borehole, north Yorkshire, England. *Rev. Palaeobot. Palynol.* **1988**, *56*, 313–326. [[CrossRef](#)]
33. Borges, M.E.N.; Riding, J.B.; Fernandes, P.; Matos, V.; Pereira, Z. Callovian (Middle Jurassic) dinoflagellate cysts from the Algarve Basin, southern Portugal. *Rev. Palaeobot. Palynol.* **2012**, *170*, 40–56. [[CrossRef](#)]
34. Riding, J.B. Dinoflagellate cyst stratigraphy of the Nettleton Bottom Borehole (Jurassic: Hettangian to Kimmeridgian), Lincolnshire, England. *Proc. Yorks. Geol. Soc.* **1987**, *46*, 231–266. [[CrossRef](#)]
35. Smelror, M.; Leereveld, H. Dinoflagellate and acritarch assemblages from the late Bathonian to Early Oxfordian of Montagne Crussol, Rhone Vally, Southern France. *Palynology* **1989**, *13*, 121–141. [[CrossRef](#)]
36. Poulsen, N.E. Dinoflagellate cysts from marine Jurassic Deposits of Denmark and Poland. *Am. Assoc. Stratigr. Palynol. Contrib. Ser.* **1996**, *31*, 1–227.
37. Borges, M.E.N.; Riding, J.B.; Fernandes, P.; Pereira, Z. The Jurassic (Pliensbachian to Kimmeridgian) palynology of the Algarve Basin and the Carrapateira outlier, southern Portugal. *Rev. Palaeobot. Palynol.* **2011**, *163*, 190–204. [[CrossRef](#)]
38. Aboul Ela, N.M.; El-Shamma, A.A. Palynostratigraphy of the middle-upper Jurassic rocks in El-Giddi borehole, north Sinai, Egypt. *Acta Univ. Carol. Geogr.* **1997**, *41*, 47–55.

39. Mafi, A.; Ghasemi-Nejad, E.; Ashouri, A.; Vahidi-Nia, M. Dinoflagellate cysts from the Upper Bajocian–Lower Oxfordian of the Dalichai Formation in Binalud Mountains (NE Iran): Their biostratigraphical and biogeographical significance. *Arab. J. Geosci.* **2013**, *7*, 3683–3692. [CrossRef]
40. Riding, J.B.; Mariani, E.; Fensome, R.A. A review of the Jurassic dinoflagellate cyst genus *Gonyaulacysta* Deflandre 1964 emend. *Nov. Rev. Palaeobot. Palynol.* **2022**, *299*, 104605. [CrossRef]
41. Woollam, R.; Riding, J.B. Dinoflagellate cyst zonation of the English Jurassic. *Inst. Geol. Sci. Lond.* **1983**, *83*, 1–42.
42. Thusu, B.; Vander Eem, J.G.A.; El Mehdawi, A.; Bu-Argoub, F. Jurassic-early Cretaceous palynostratigraphy in northeast Libya. In *Subsurface Palynostratigraphy of Northeast Libya*; El-Arnauti, A., Owens, B., Thusu, B., Eds.; Garyounis University Publication: Benghazi, Libya, 1988; pp. 171–214.
43. Aboul Ela, N.M.; Mahrous, H.A.R. Bathonian dinoflagellate cysts from the subsurface Jurassic of north Western Desert, Egypt. MERC Ain Shams University. *Earth Sci. Ser.* **1990**, *4*, 95–111.
44. Thusu, B.; Vigran, J.O. Middle-Late Jurassic (Late Bathonian-Tithonian) palynomorphs. *J. Micropalaeontol.* **1985**, *4*, 113–130. [CrossRef]
45. Rauscher, R.; Schmitt, J.P. Recherches palynologiques dans le jurassique d’Alsace (France). *Rev. Palaeobot. Palynol.* **1990**, *62*, 107–156. [CrossRef]
46. Shahin, A.M.; El Beialy, S.Y. Microfossils from Middle Juraassic Shusha Formation of the Gebel El Maghara, Sinai, Egypt. *Neues Jahrb. Für Geol. Und Paläontologie Abh.* **1989**, *9*, 560–576. [CrossRef]
47. Courtinat, B. Les organoclasts des formations lithologiques du Malm dans le Jura Méridional. Systematique, biostratigraphie et éléments d’interprétation Paléoécologique. *Trav. Et Doc. Des Lab. De Géologie De Lyon* **1989**, *105*, 150–361.
48. Dürr, G. Palynostratigraphie des Kimmeridgium und Tithonium von Süddeutschland und Korrelation mit borealen Floren. *Tübinger Mikropaläontologische Mitt.* **1988**, *5*, 1–159.
49. El Shamma, A.A.; Obied, F.L.; Abu Saima, M.M. Palynostratigraphy of some subsurface Jurassic-lower cretaceous rocks in northern Western Desert. *Egypt. J. Geol.* **2001**, *45*, 567–605.
50. El Beialy, S.Y.; Zalat, A.; Ali, A.S. The palynology of the Bathonian-early Oxfordian succession in the East Faghur-1 well, Western Desert, Egypt. *Egypt. J. Palaeontol.* **2002**, *2*, 399–414.
51. Thusu, B. Aptian to Toarcian dinoflagellate cysts from Arctic Norway. In *Distribution of Biostratigraphically Diagnostic Dinoflagellate Cysts and Miospores from the Northwest European Continental Shelf and Adjacent Areas*. 100; Thusu, B., Ed.; Continental Shelf Institute Publication, 1978; pp. 61–95. Available online: <https://pascal-francis.inist.fr/vibad/index.php?action=getRecordDetail&idt=6373089> (accessed on 7 March 2023).
52. Riding, J.; Penn, I.E.; Woollam, R. Dinoflagellate cysts from the type area of the Bathonian Stage (Middle Jurassic; England). *Rev. Palaeobot. Palynol.* **1985**, *45*, 149–169. [CrossRef]
53. Hengreen, G.F.W.; De Boer, K.F.; Romein, B.J.; Lissenberg, T.; Wijker, N.C. Middle Callovian beds in the Achterhoek, eastern Netherlands. *Meded. Rijks Geol. Dienst* **1984**, *37*, 1–29.
54. Mahmoud, M.S. Middle jurassic and lower cretaceous dinocyst and miospores from the agnes-1 well, Western Desert, Egypt. *Neues Jahrb. Geol. Palaontol. Abhand.* **1991**, *11*, 693–706. [CrossRef]
55. Dodekova, L. New Upper Bathonian dinoflagellate cysts from northeastern Bulgaria. *Bulg. Akad. Na Nauk. Paleontol. Stratigr. I Litol.* **1975**, *2*, 17–34.
56. Smelror, M.; Arhus, N.; Melenndez, G.; Lardies, M.D. A reconnaissance study of the Bathonian to Oxfordian (Jurassic) dinoflagellates and Acritarchs from the Zaragoza region (NE Spain) and Figueira da Foz (Portugal). *Rev. Esp. Micropaleontol.* **1991**, *23*, 47–82.
57. Prauss, M. Dinozysten-stratigraphie und palynofazies im oberen Lias und Dogger von NW-Deutschland. *Palaeontograph. Abt. B* **1989**, *214*, 1–124.
58. Naim, G.; Enani, N.; Aly, S.M. Stratigraphy and structural setting of the Jurassic boreholes in Gabal Maghara, Sinai. *Annu. Geol. Surv. Egypt* **1990**, *16*, 205–214.
59. Riding, J.B.; Fedorova, V.A.; Ilyina, V.I. Jurassic and lowermost Cretaceous dinoflagellate cyst biostratigraphy of the Russian Platform and northern Siberia, Russia. *Am. Assoc. Stratigr. Palynol. Contrib. Ser.* **1999**, *36*, 179.
60. Bailey, D.A.; Partington, M. Some Middle Jurassic dinocysts from the Brent Group of the northern North Sea. *J. Micropalaeontol.* **1991**, *9*, 245–252. [CrossRef]
61. Wood, S.E.; Gorin, G.E. Sedimentary organic matter in distal clinofolds of Miocene slope sediments; Site 903 of ODP Leg 150, offshore New Jersey (U.S.A.). *J. Sediment. Res.* **1998**, *68*, 856–868. [CrossRef]
62. Batten, D.J. Palynofacies and petroleum potential. In *Palynology: Principles and Applications*; Jansonius, J., McGregor, D.C., Eds.; American Association of Stratigraphic Palynologists Foundation: Salt Lake City, UT, USA, 1996; pp. 1065–1084.
63. Batten, D.J. Palynofacies analysis. In *Fossil plants and Spores: Modern Techniques*; Jones, T.P., Rowe, N.P., Eds.; Geological Society: London, UK, 1999; pp. 194–198.
64. Mendonça Filho, J.G.; Menezes, T.R.; Mendonça, J.O.; Oliveira, A.D.; Silva, T.F.; Rondon, N.F.; Da Silva, F.S. Organic facies: Palynofacies and organic geochemistry approaches. In *Geochemistry–Earth’s System Processes*; Panagiotaras, D., Ed.; InTech: Rang-Du-Fliers, France, 2012; pp. 211–248.

65. McCarthy, F.M.G.; Katz, M.E.; Kotthoff, U.; Drljepan, M.; Zanatta, R.; Williams, R.H.; Browning, J.V.; Hesselbo, S.P.; Bjerrum, C.J.; Miller, K.G.; et al. Eustatic control of New Jersey margin architecture: Palynological evidence from IODP Expedition 313. *Geosphere* **2013**, *9*, 1457–1487. [[CrossRef](#)]
66. Mansour, A.; Tahoun, S.S.; Gentzis, T.; Elewa, A.M.T. The marine palynology of the Upper Cretaceous Abu Roash 'A' Member in the BED 2-3 borehole, Abu Gharadig Basin, Egypt. *Palynology* **2020**, *44*, 167–186. [[CrossRef](#)]
67. Mansour, A.; Gentzis, T.; Tahoun, S.S.; Ahmed, M.S.; Wagreich, M.; Carvajal-Ortiz, H.; Neumann, J.; Radwan, A.E. Paleoenvironmental, paleoclimatic, and organic matter assessment of the hybrid Kharita Formation (Albian) in the Abu Gharadig Basin, Egypt: Integration between palynology, organic petrography, and organic geochemistry. *Mar. Pet. Geol.* **2023**, *148*, 106072. [[CrossRef](#)]
68. Steffen, D.; Gorin, G. Sedimentology of organic matter in upper Tithonian-Berriasian deep-sea carbonates of southeast France: Evidence of eustatic control. In *Source Rocks in Sequence Stratigraphic Framework*; Katz, B., Prott, L., Eds.; American Association of Petroleum Geologists: Washington, DC, USA, 1993; pp. 49–65.
69. Wicander, R.; Playford, G. Acritarchs and spores from the Upper Devonian Lime Creek Formation, Iowa, USA. *Micropaleontology* **1985**, *31*, 97–138. [[CrossRef](#)]
70. Wicander, R.; Playford, G. Marine and terrestrial palynofloras from transitional Devonian-Mississippian strata, Illinois Basin, USA. *Bol. Geol. Miner.* **2013**, *124*, 589–637.
71. Brinkhuis, H. Late Eocene to early Oligocene dinoflagellate cysts from the Priabonian type-area (Northeast Italy): Biostratigraphy and paleoenvironmental interpretation. *Palaeogeogr. Palaeoclimatol. Palaeoecol.* **1994**, *107*, 121–163. [[CrossRef](#)]
72. Lister, J.K.; Batten, D.J. Stratigraphic and palaeoenvironmental distribution of Early Cretaceous dinoflagellate cysts in the Hurlands farm borehole, West Sussex, England. *Palaeontogr. Abt. B* **1988**, *210*, 9–89.
73. Dale, B. Dinoflagellate resting cysts: "benthic plankton". In *Survival Strategies of the Algae*; Fryxell, G.A., Ed.; Cambridge University Press: Cambridge, UK, 1983; pp. 69–136.

Disclaimer/Publisher's Note: The statements, opinions and data contained in all publications are solely those of the individual author(s) and contributor(s) and not of MDPI and/or the editor(s). MDPI and/or the editor(s) disclaim responsibility for any injury to people or property resulting from any ideas, methods, instructions or products referred to in the content.